Title: GW190521 may be an intermediate mass ratio inspiral

Speakers: Alexander Nitz, Collin Capano

Series: Strong Gravity

Date: November 05, 2020 - 1:00 PM

URL: http://pirsa.org/20110043

Abstract: Abstract and Zoom Link: TBD

Understanding the heaviest gravitational-wave observation: Could GW190521 be an intermediate mass ratio inspiral?

Alex Nitz & Collin Capano
Albert Einstein Institute
Hannover, Germany

arXiv:2010.12558

arXiv:2010.12558v2 [astro-ph.HE] 3 Nov 2020

Draft version November 4, 2020
Typeset using LaTeX **twocolumn** style in AASTeX63

GW190521 may be an intermediate mass ratio inspiral

Alexander H. Nitz[1,2] and Collin D. Capano[1,2]

[1] Max-Planck-Institut für Gravitationsphysik (Albert-Einstein-Institut), D-30167 Hannover, Germany
[2] Leibniz Universität Hannover, D-30167 Hannover, Germany

ABSTRACT

GW190521 is the first confident observation of a binary black hole merger with total mass $M > 100\,\mathrm{M}_\odot$. Given the lack of observational constraints at these masses, we analyze GW190521 considering two different priors for the binary's masses: uniform in mass ratio and source-frame total mass, and uniform in source-frame component masses. For the uniform in mass-ratio prior, we find that the component masses are $m_1^{\rm src} = 168^{+15}_{-61}\,\mathrm{M}_\odot$ and $m_2^{\rm src} = 16^{+33}_{-3}\,\mathrm{M}_\odot$. The uniform in component-mass prior yields a bimodal posterior distribution. There is a low-mass-ratio mode ($q < 4$) with $m_1^{\rm src} = 100^{+17}_{-18}\,\mathrm{M}_\odot$ and $m_2^{\rm src} = 57^{+17}_{-16}\,\mathrm{M}_\odot$ and a high-mass-ratio mode ($q \geq 4$) with $m_1^{\rm src} = 166^{+16}_{-35}\,\mathrm{M}_\odot$ and $m_2^{\rm src} = 16^{+14}_{-3}\,\mathrm{M}_\odot$. Although the two modes have nearly equal posterior probability, the maximum-likelihood parameters are in the high-mass ratio mode, with $m_1^{\rm src} = 171\,M_\odot$ and $m_2^{\rm src} = 16\,M_\odot$, and a signal-to-noise ratio of 16. These results are consistent with the proposed "mass gap" produced by pair-instability in supernova. Our results are inconsistent with those published in Abbott et al. (2020b). We find that a combination of the prior used and the constraints applied may have prevented that analysis from sampling the high-mass-ratio mode. An accretion flare in AGN J124942.3+344929 was observed in possible coincidence with GW190521 by the Zwicky Transient Facility (ZTF). We report parameters assuming a common origin; however, the spatial agreement of GW190521 and the EM flare alone does not provide convincing evidence for the association ($\ln \mathcal{B} \gtrsim -4$).

Keywords: gravitational waves — black holes — compact binary stars

1. INTRODUCTION

Gravitational-wave astronomy began with the observation of GW150914 (Abbott et al. 2016) by the twin LIGO-Hanford and Livingston observatories (Aasi et al. 2015) with the merger of two $\sim 30\mathrm{M}_\odot$ black holes, significantly heavier than previously known black holes in X-ray binaries (Corral-Santana et al. 2016). These heavy binary black holes (BBHs) opened a new window into stellar evolution (Taylor & Gerosa 2018; Dvorkin et al. 2018; Piran & Hotekezaka 2020) and even sparked renewed interest in primordial black holes as a component of dark matter (Green & Kavanagh 2020; Nitz & Wang 2020; Abbott et al. 2019a). Since then, the Virgo observatory (Acernese et al. 2015) has joined the growing worldwide observatory network and over a dozen binary black hole mergers have been observed (Nitz et al. 2019a,b, 2020; Venumadhav et al. 2019a,b; Zackay et al. 2019; Abbott et al. 2019b), with many additional candidates awaiting publication (LVC 2019).

With the exception of the marginal BBH candidates GW151205 and 170817+03:02:46UTC (Nitz et al. 2019b; Zackay et al. 2019), all prior confident detections were consistent with sources in which both component black holes have mass less than $50\mathrm{M}_\odot$ (Abbott et al. 2019c). This observed limit may hint at the existence of an upper mass gap (Abbott et al. 2019c; Roulet et al. 2020). Formation models which include the effects of pulsational pair instability supernovae (PPISNe) or pair-instability supernovae (PISNe) in stellar evolution preclude the direct formation of a black hole with remnant mass ~ 50–$120\,\mathrm{M}_\odot$ (Yoshida et al. 2016; Woosley 2017; Belczynski et al. 2016; Marchant et al. 2019; Woosley 2019; Stevenson et al. 2019; van Son et al. 2020).

On May 21st, 2019 at 03:02:29 UTC, GW190521 was detected by the PyCBC Live low-latency analysis (Nitz et al. 2018a; Dal Canton et al. 2020), producing a 765 deg^2 Bayestar sky localization (Singer & Price 2016). Continued monitoring of the low-latency localiza-

Corresponding author: Alexander H. Nitz
alex.nitz@aei.mpg.de

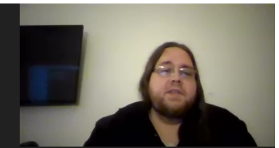

Outline

- Gravitational-wave Astronomy
  - summary of current observations
- Discovery of GW190521
  - Possible EM counterpart
- GW Bayesian Inference
- Unexpected Results
- What are the parameters of GW190521
  - implications for formation scenarios
  - implications for EM flare coincidence
- Comparisons to prior results and sources of systematic error

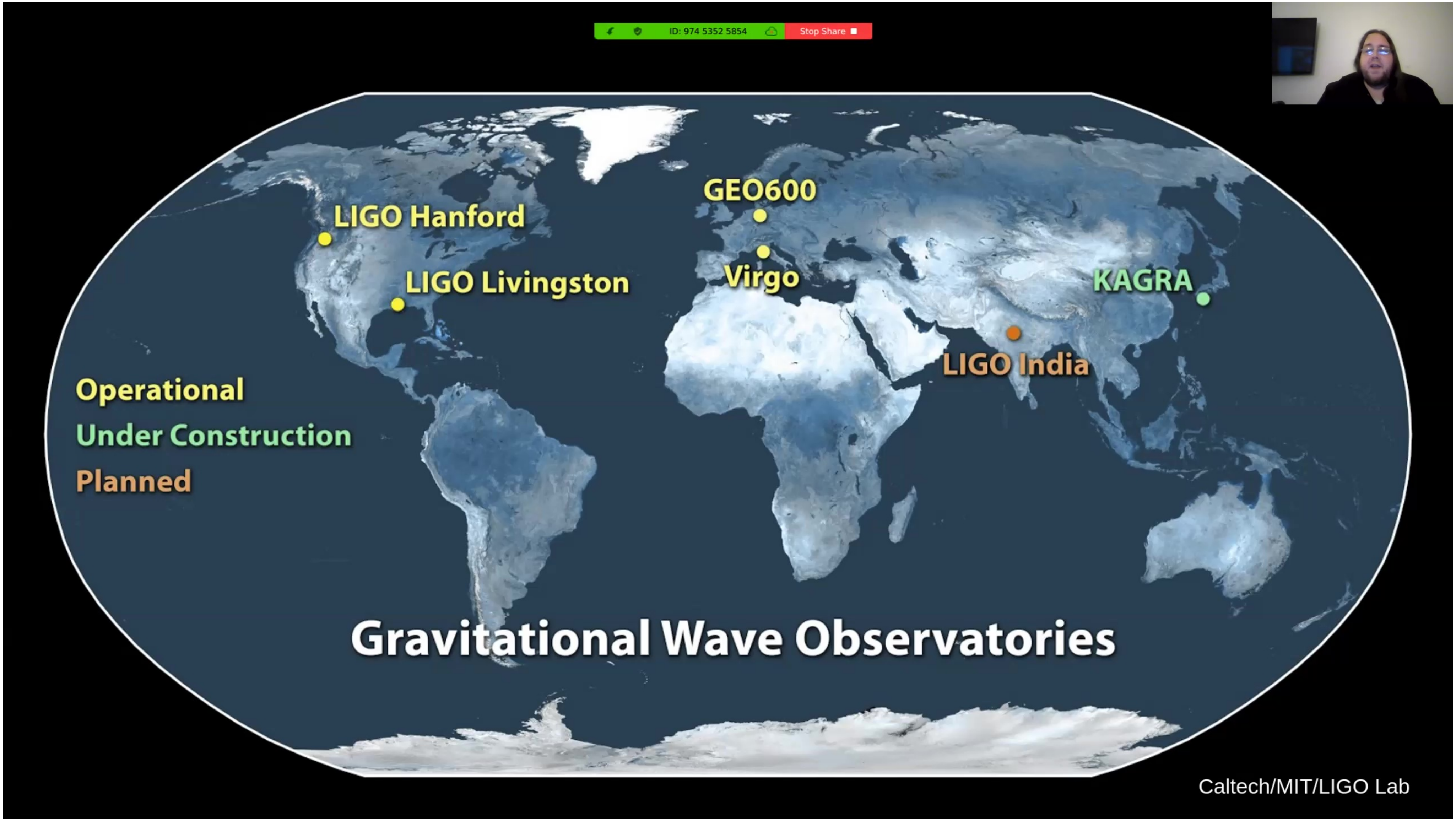
ID: 974 5352 5854
Stop Share
GEO600
LIGO Hanford
LIGO Livingston
Virgo
KAGRA
LIGO India
Operational
Under Construction
Planned
Gravitational Wave Observatories
Caltech/MIT/LIGO Lab

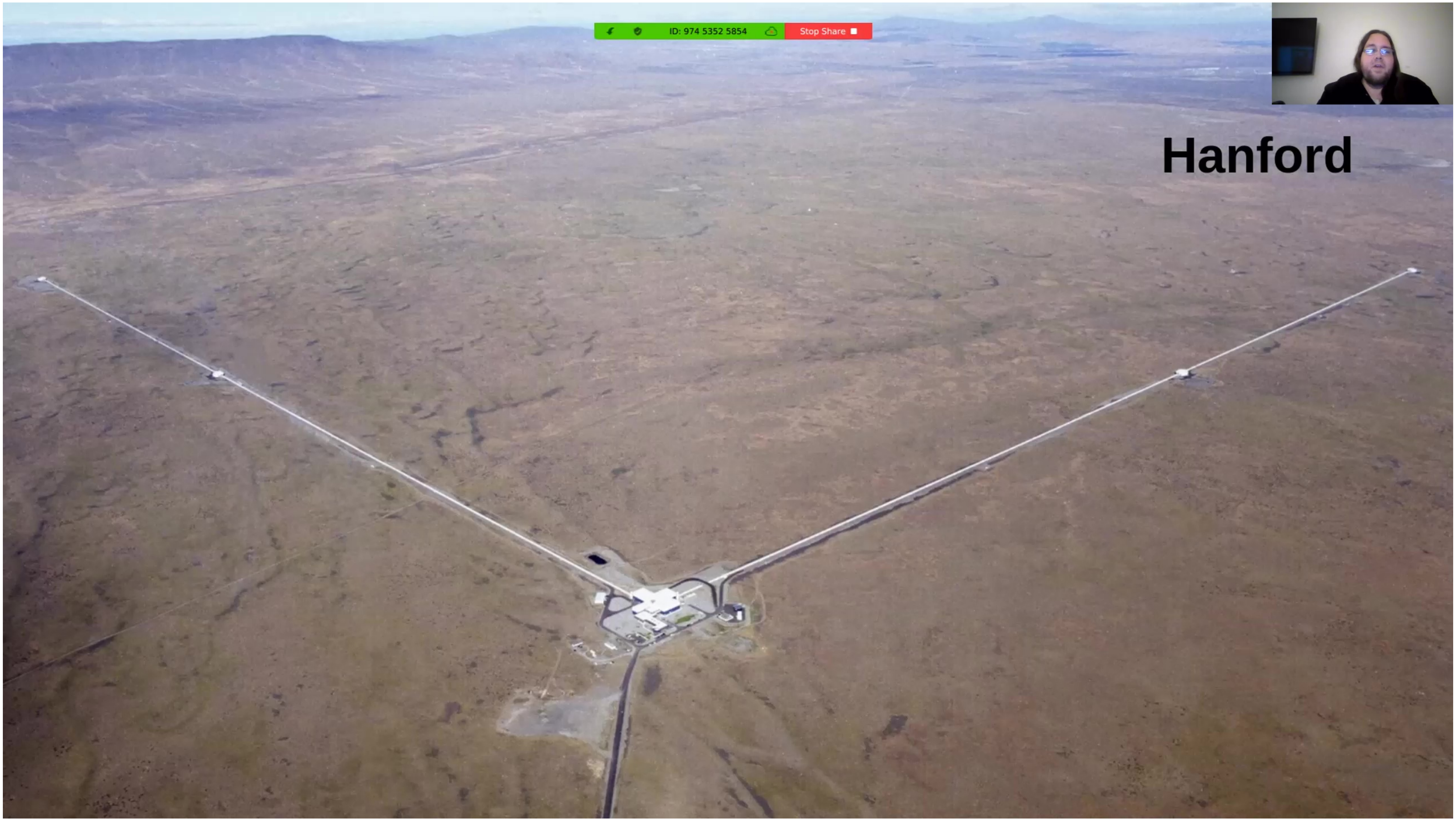
ID: 974 5352 5854
Stop Share
Hanford

ID: 974 5352 5854 Stop Share

Advanced LIGO & Virgo Observing runs

- First observing run (O1): September 12, 2015 - January 19, 2016
  - Hanford and Livingston only
  - First detection of gravitational wave, GW150914; from a binary black hole merger
- Second observing run (O2): November 30, 2016 - August 25,2017
  - Virgo joins the network
  - First detection of binary neutron star merger GW170817; also first multimessenger observation
- Third observing run (O3): two periods
  - **O3a: April 1, 2019 - October 1, 2019**
  - O3b: November 1, 2019 - March 27, 2020

ID: 974 5352 5854 Stop Share

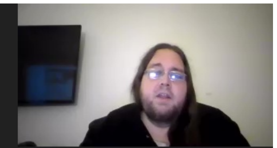

A quickly growing population of observations

https://arxiv.org/abs/2010.14527

- Period from April - Oct 2019 (only ~half the data set)

- ~ 50 observed mergers, vast majority are binary black holes
    - Only a single "BNS" observed

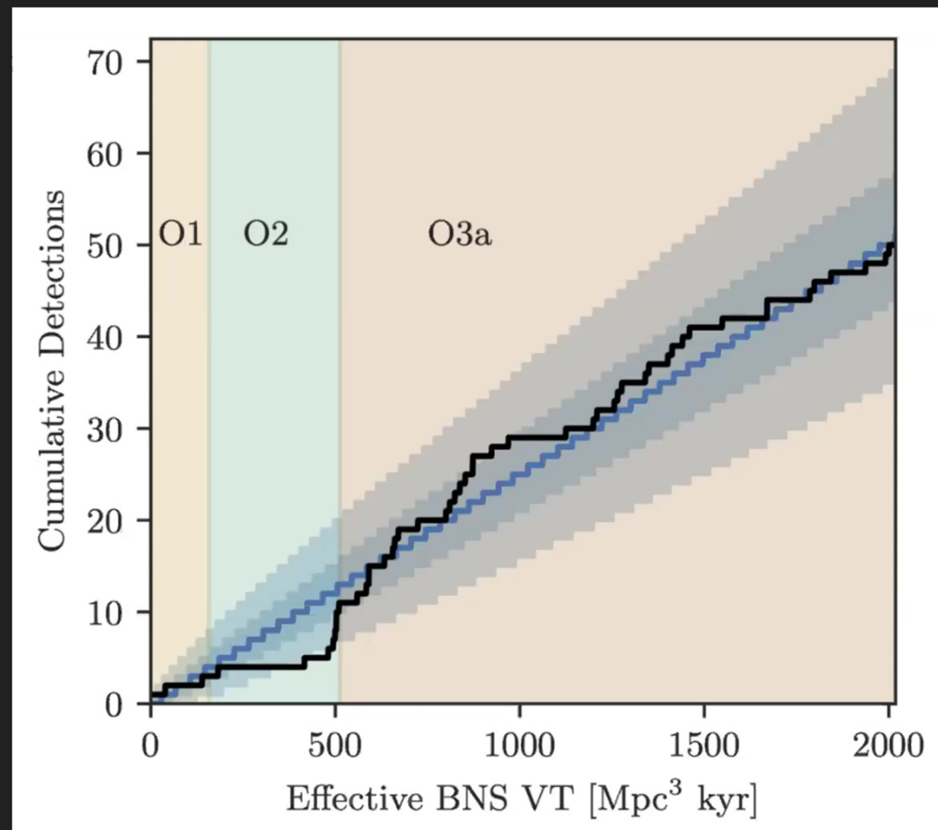

LVC, GWTC-2, https://arxiv.org/abs/2010.14527

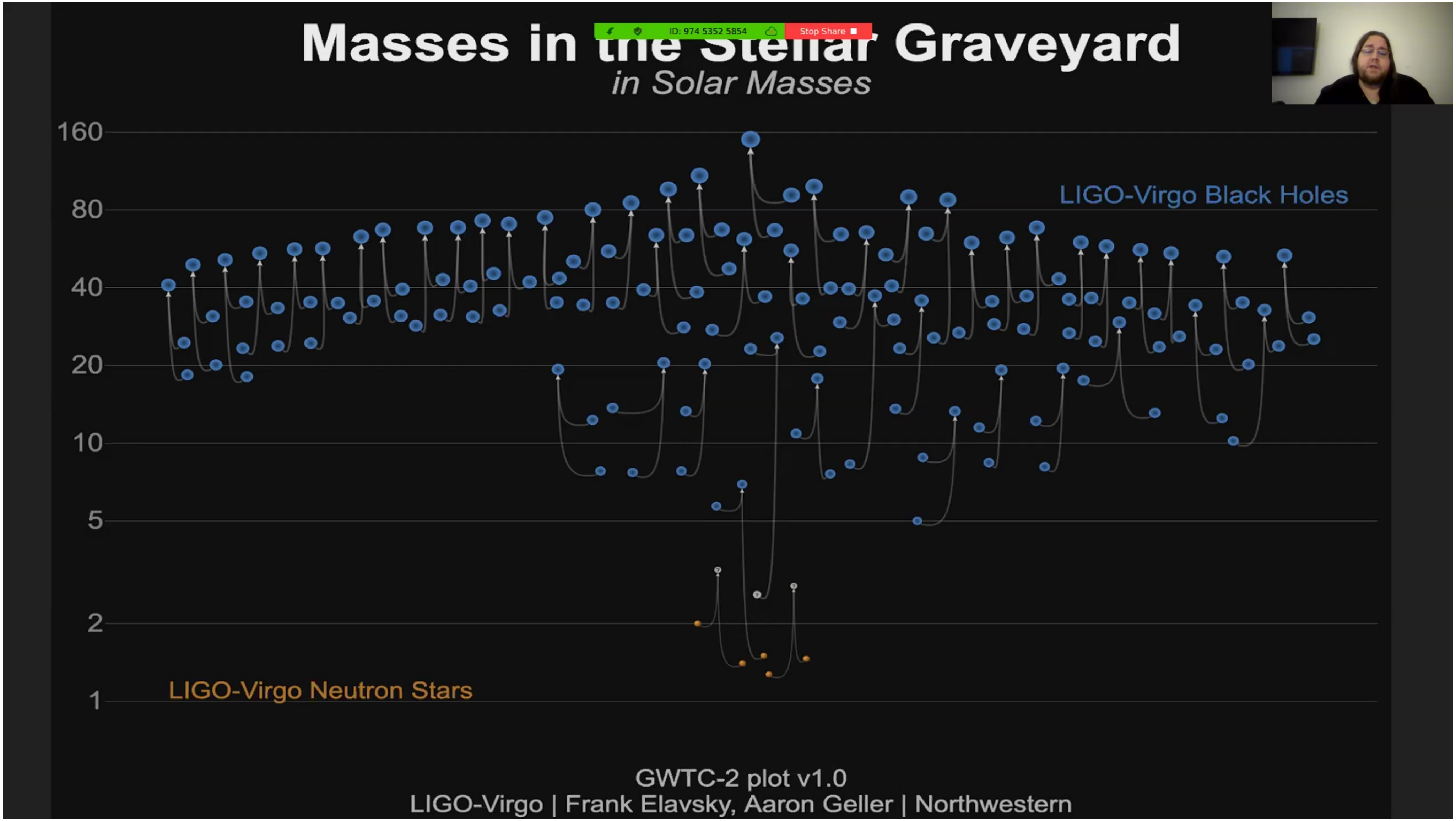
Masses in the Stellar Graveyard
in Solar Masses
ID: 974 5352 5854
Stop Share
160
80
40
20
10
5
2
1
LIGO-Virgo Black Holes
LIGO-Virgo Neutron Stars
GWTC-2 plot v1.0
LIGO-Virgo | Frank Elavsky, Aaron Geller | Northwestern

Formation Scenarios for Binary Black Hole Mergers

"Isolated Binaries" — "Dynamical"

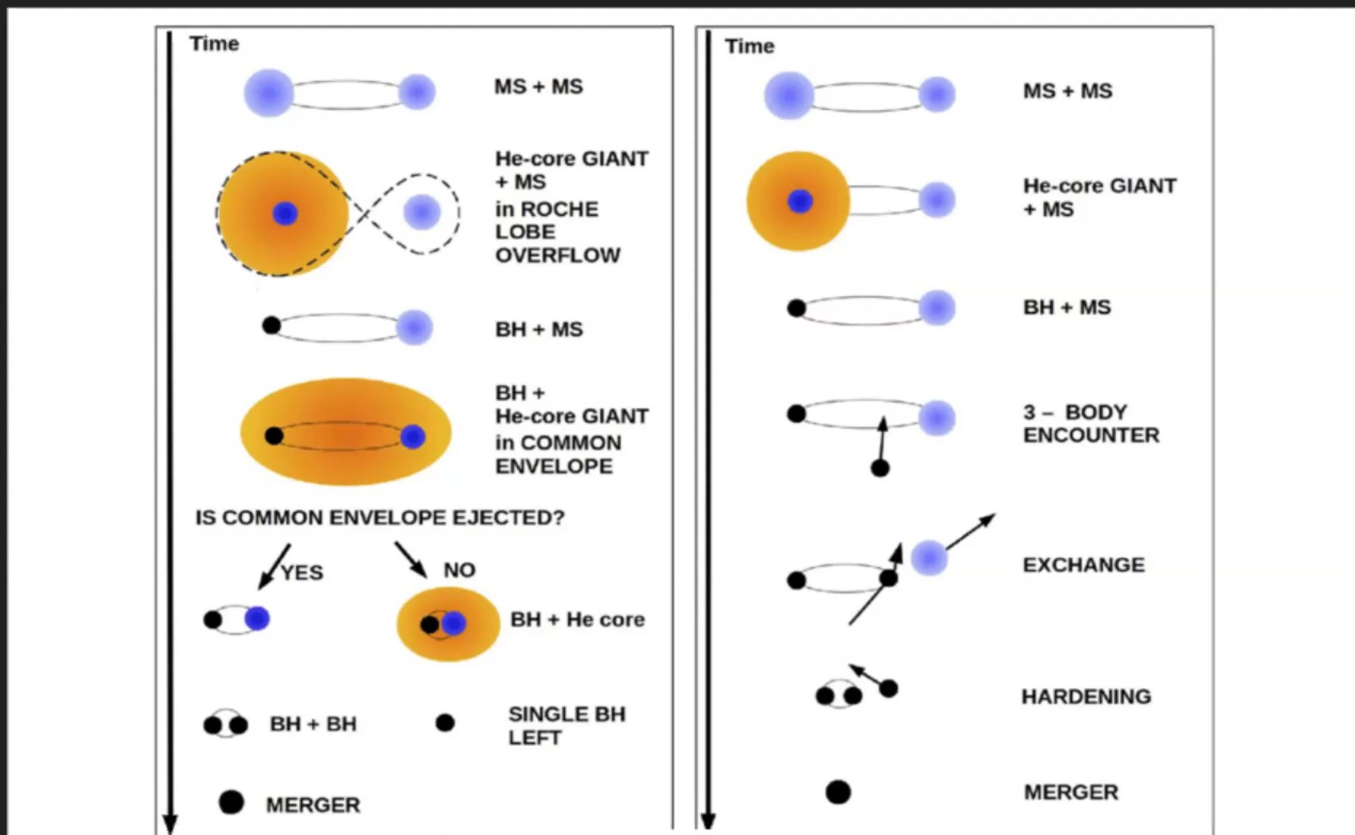

Michela Mapelli, Astron. Space Sci., 09 July 2020

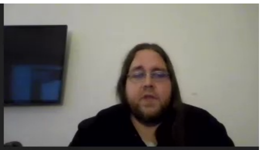

Discovery of GW190521

GW190521

Observed on May 21, 2019 at 03:02:29 UTC

- Initially identified by PyCBC Live CBC search and generic cWB search, confirmed by several others
- Reported and sent to observers in O(minutes) as S190521g
- $\sim 800\ \text{deg}^2$ sky localization.

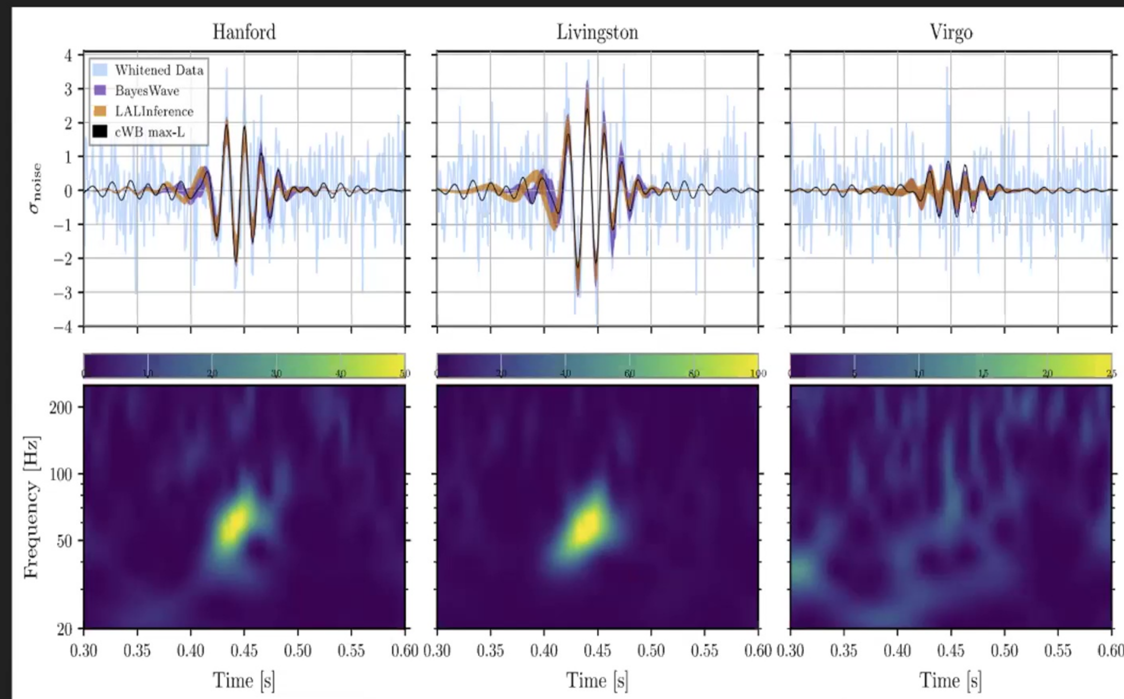

LVC, Phys. Rev. Lett. 125, 101102 (2020)

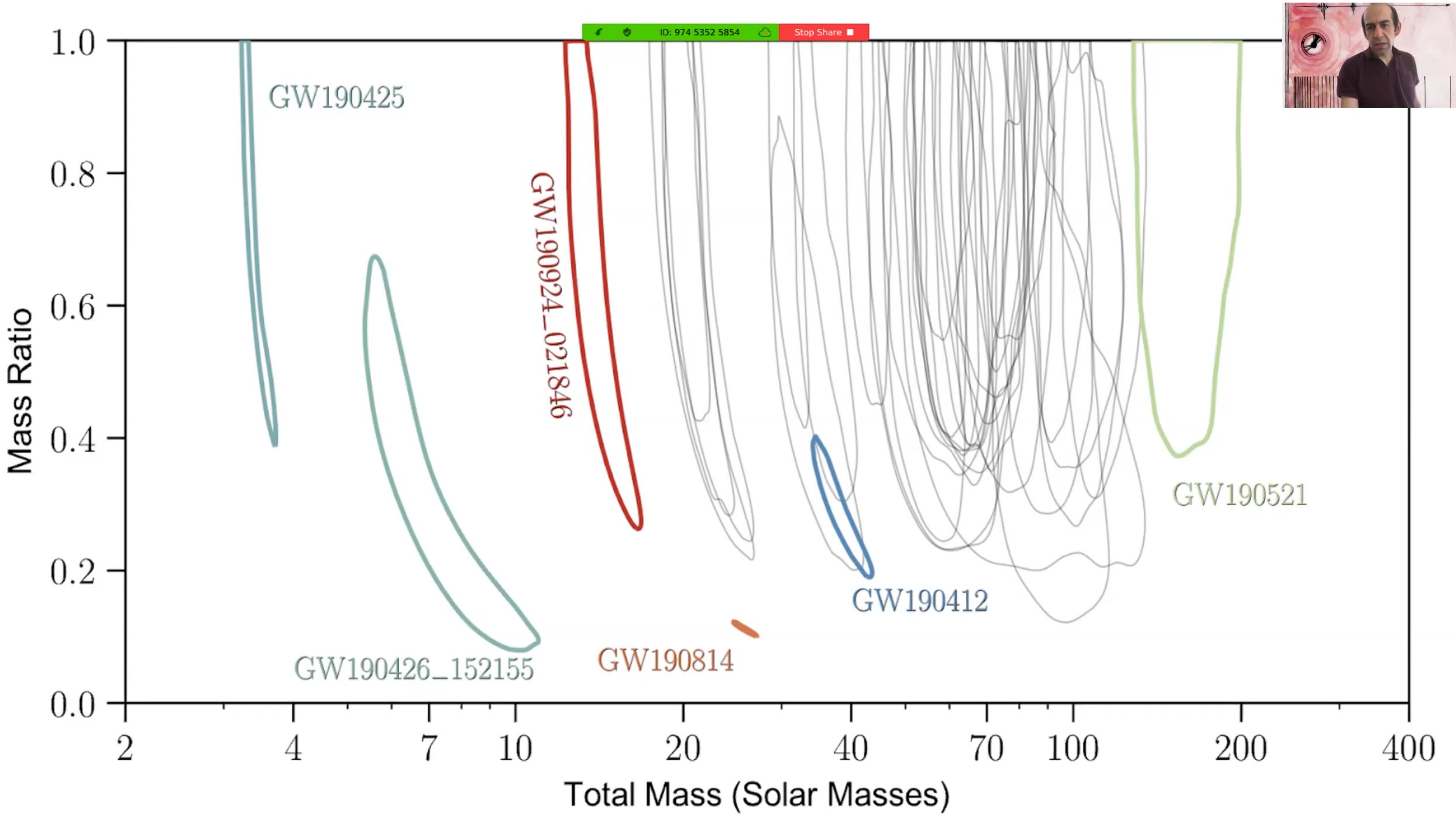

LVC, GWTC-2, https://arxiv.org/abs/2010.14527

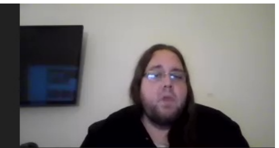

GW190521

Observed on May 21, 2019 at 03:02:29 UTC

- Initially identified by PyCBC Live CBC search and generic cWB search, confirmed by several others
- Reported and sent to observers in O(minutes) as S190521g
- ~ 800 deg^2 sky localization.

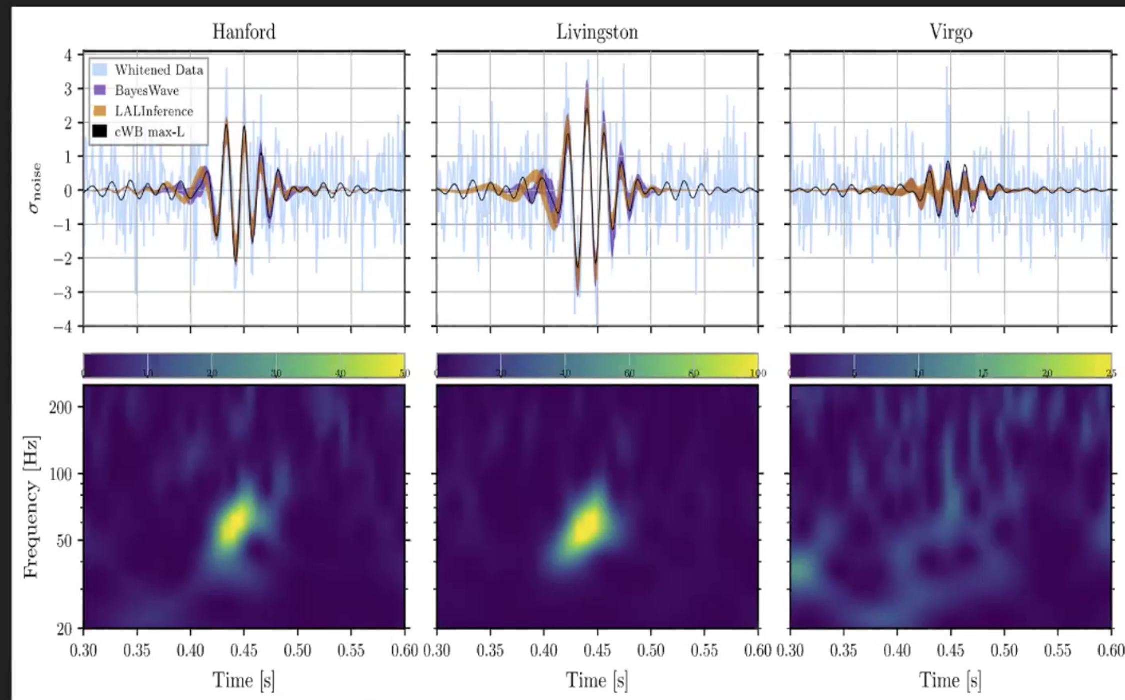

LVC, Phys. Rev. Lett. 125, 101102 (2020)

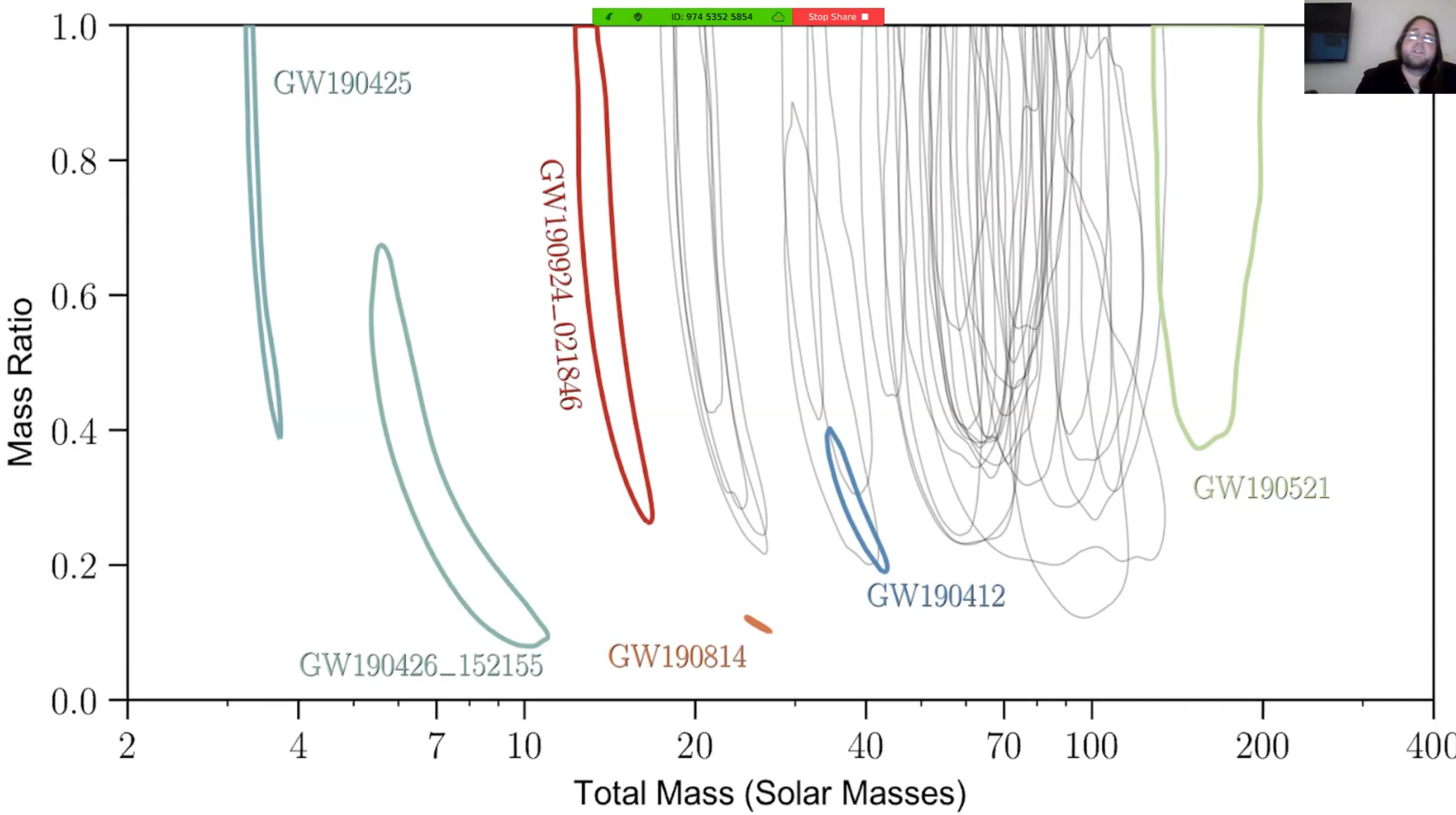

LVC, GWTC-2, https://arxiv.org/abs/2010.14527

Potential Electromagnetic Counterpart?

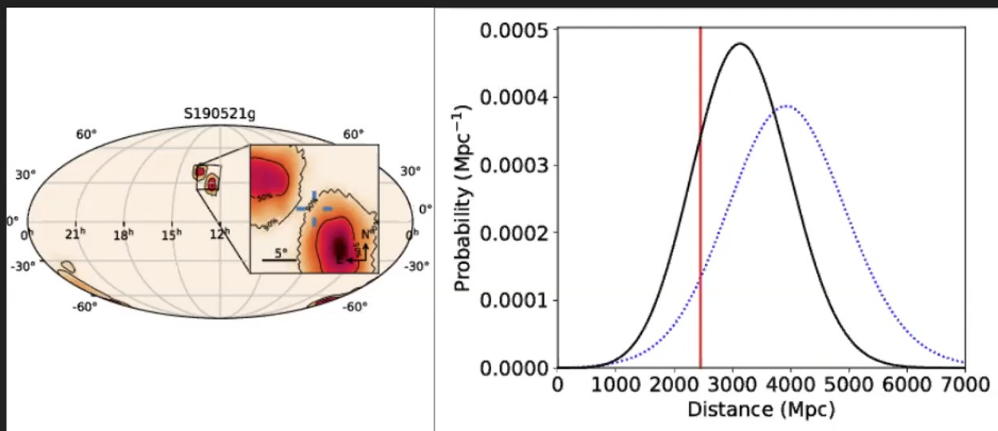

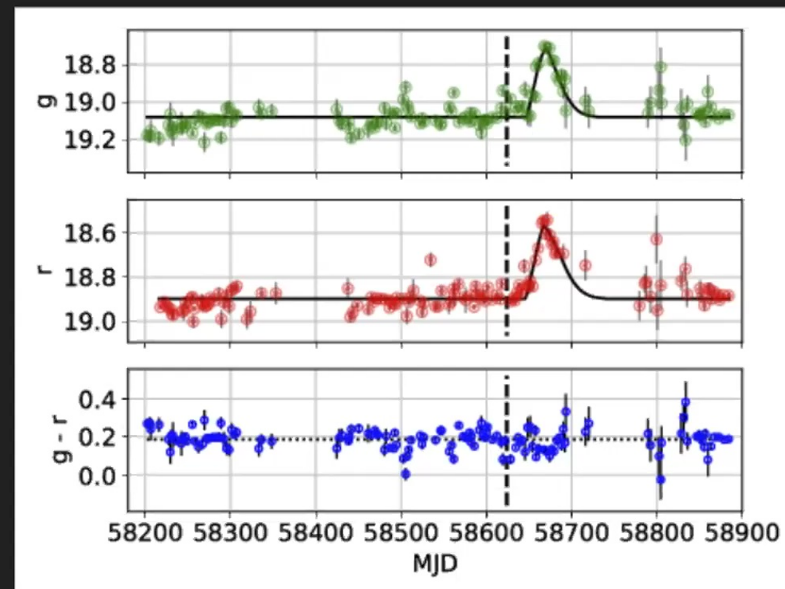

- Continued by Zwicky Transient Facility
  - EM Flare observed in spatial coincidence ~ 1 month later
  - AGN J124942.3+344929 (ZTF19abanrhr)
- The merger may have occurred within the disk of an AGN

Graham, et al. Phys. Rev. Lett. 124, 251102
https://arxiv.org/abs/2006.14122

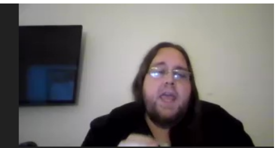

LVC: GW190521 as a hierarchical merger?

- Primary BH ~ 85 solar masses
- Secondary BH ~ 66 solar masses
- 90-99% probability that at least one BH is between 65 - 120 solar masses
  - Pair-instability Supernovae may prevent formation of BH remnants between ~50-120 solar masses
  - Suggests a possible hierarchical merger

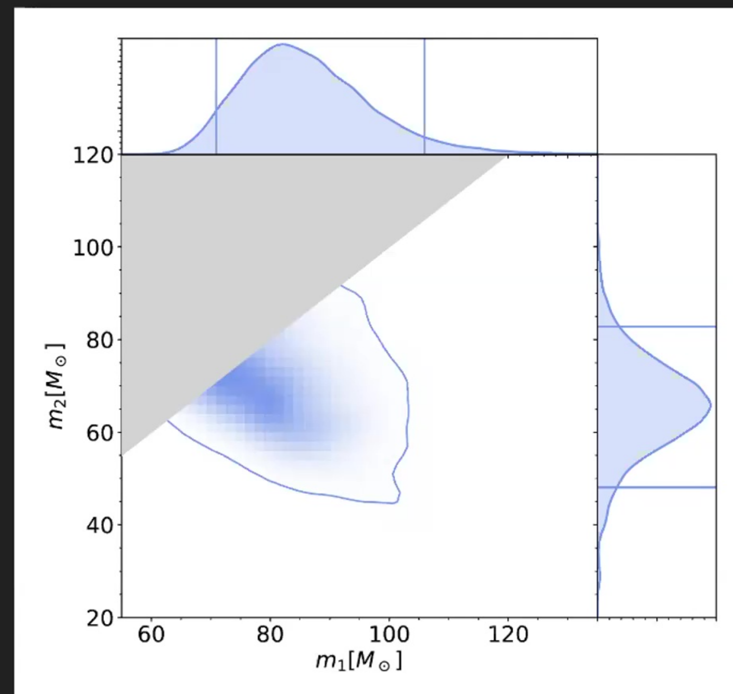

LVC, Phys. Rev. Lett. 125, 101102 (2020)

Questions

How consistent are the locations of the EM flare and GW observation?

If they are from a common source, does this affect what we infer about the source parameters?

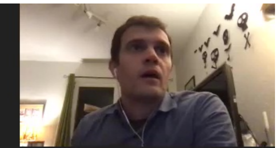

GW Bayesian Inference and Model Selection

Binary black hole parameters

Possible BBH parameters (#):

- Component masses m_1, m_2 (2)
- Dimensionless spins of components χ_1, χ_2 (6)
  - If spins are misaligned with orbital angular momentum L, get precession
- Location & orientation (6)
  - right ascension, declination, & distance
  - inclination (angle between line of sight and L at a fiducial GW frequency)
  - orbital phase & polarization
- Orbital eccentricity, but in this analysis we assume circular orbits

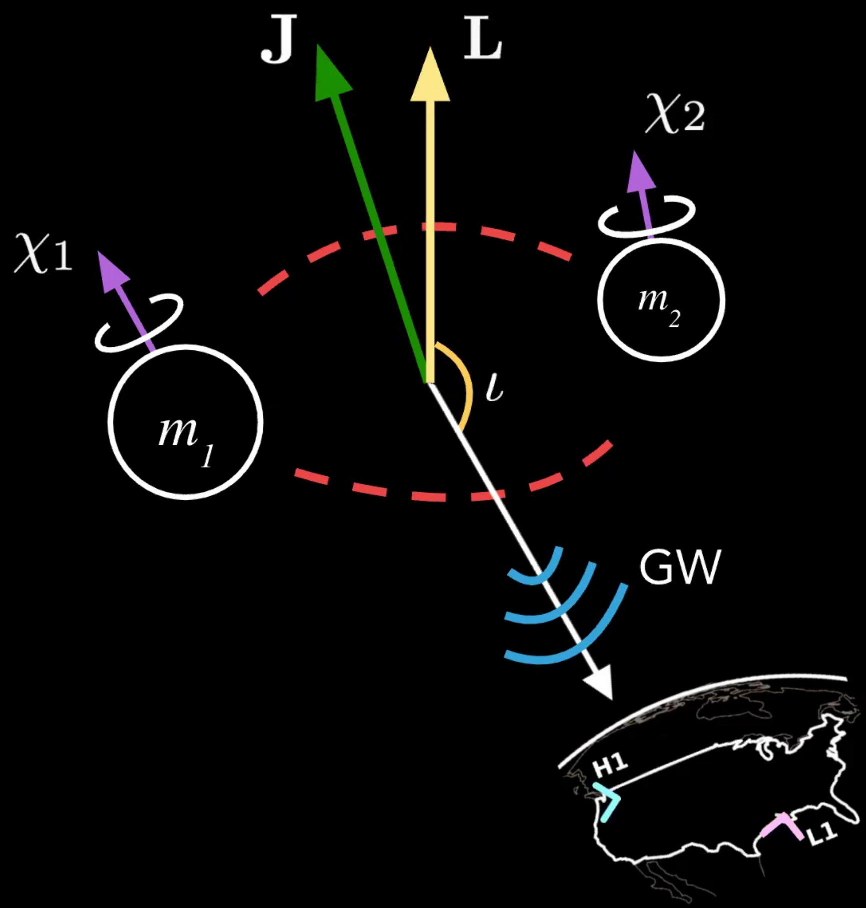

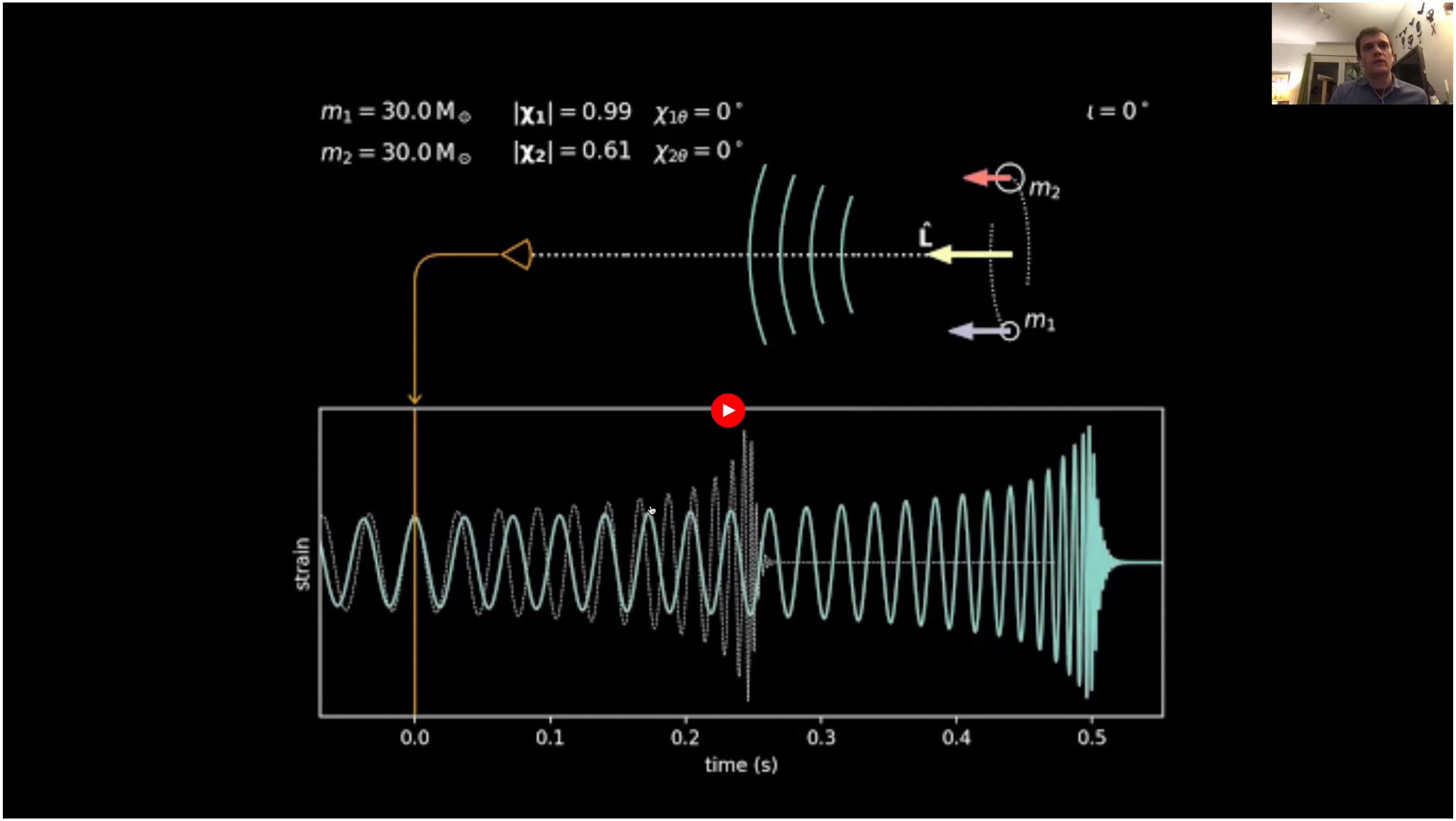

$m_1 = 30.0\,M_\odot$ $|\chi_1| = 0.99$ $\chi_{1\theta} = 0^\circ$
$m_2 = 30.0\,M_\odot$ $|\chi_2| = 0.61$ $\chi_{2\theta} = 0^\circ$
$\iota = 0^\circ$
m_2
$\hat{L}$
m_1
strain
0.0
0.1
0.2
0.3
0.4
0.5
time (s)

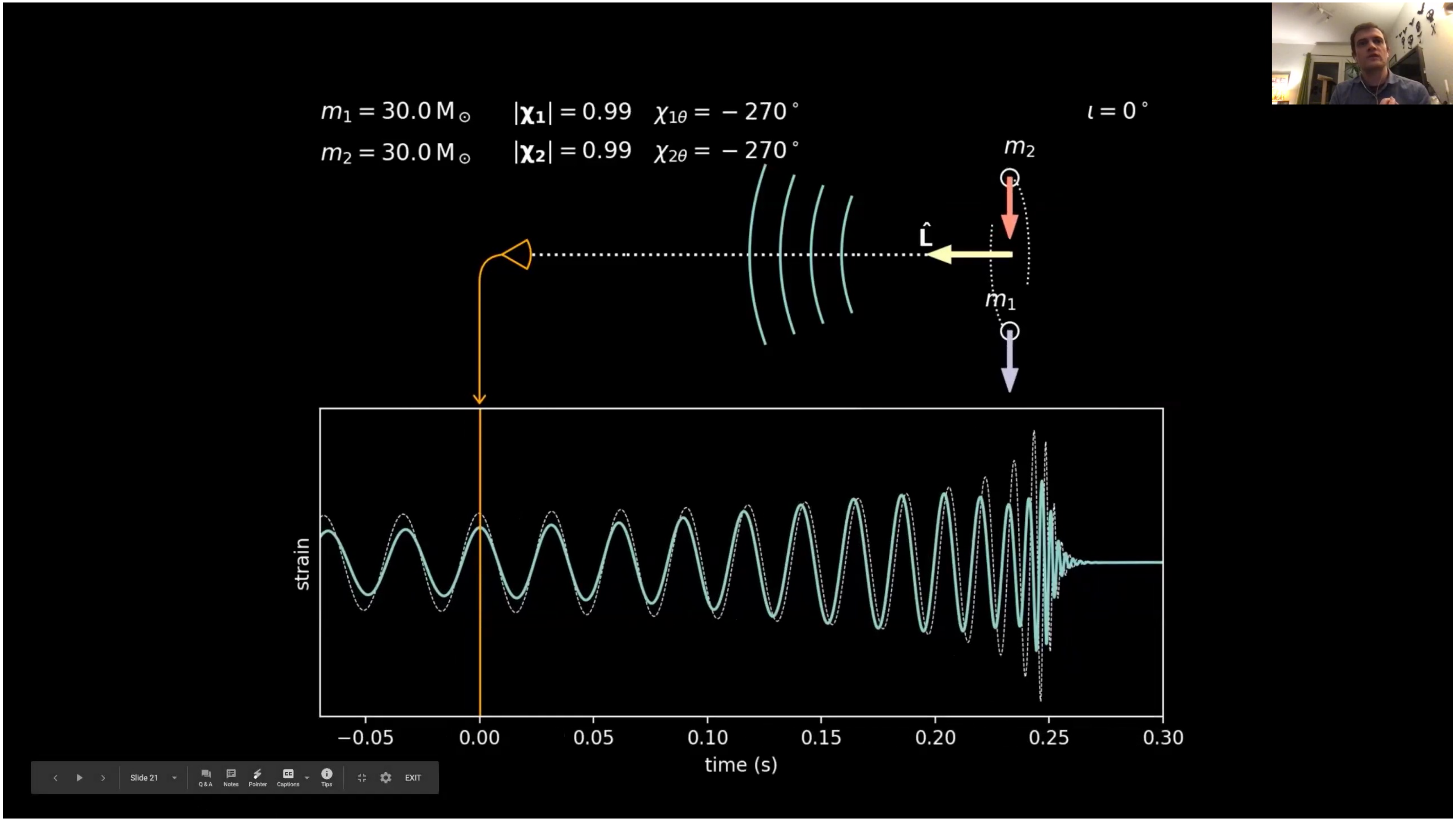

$m_1 = 30.0\,M_\odot$ $|\chi_1| = 0.99$ $\chi_{1\theta} = -270^\circ$
$m_2 = 30.0\,M_\odot$ $|\chi_2| = 0.99$ $\chi_{2\theta} = -270^\circ$
$\iota = 0^\circ$
m_2
$\hat{L}$
m_1
strain
−0.05 0.00 0.05 0.10 0.15 0.20 0.25 0.30
time (s)

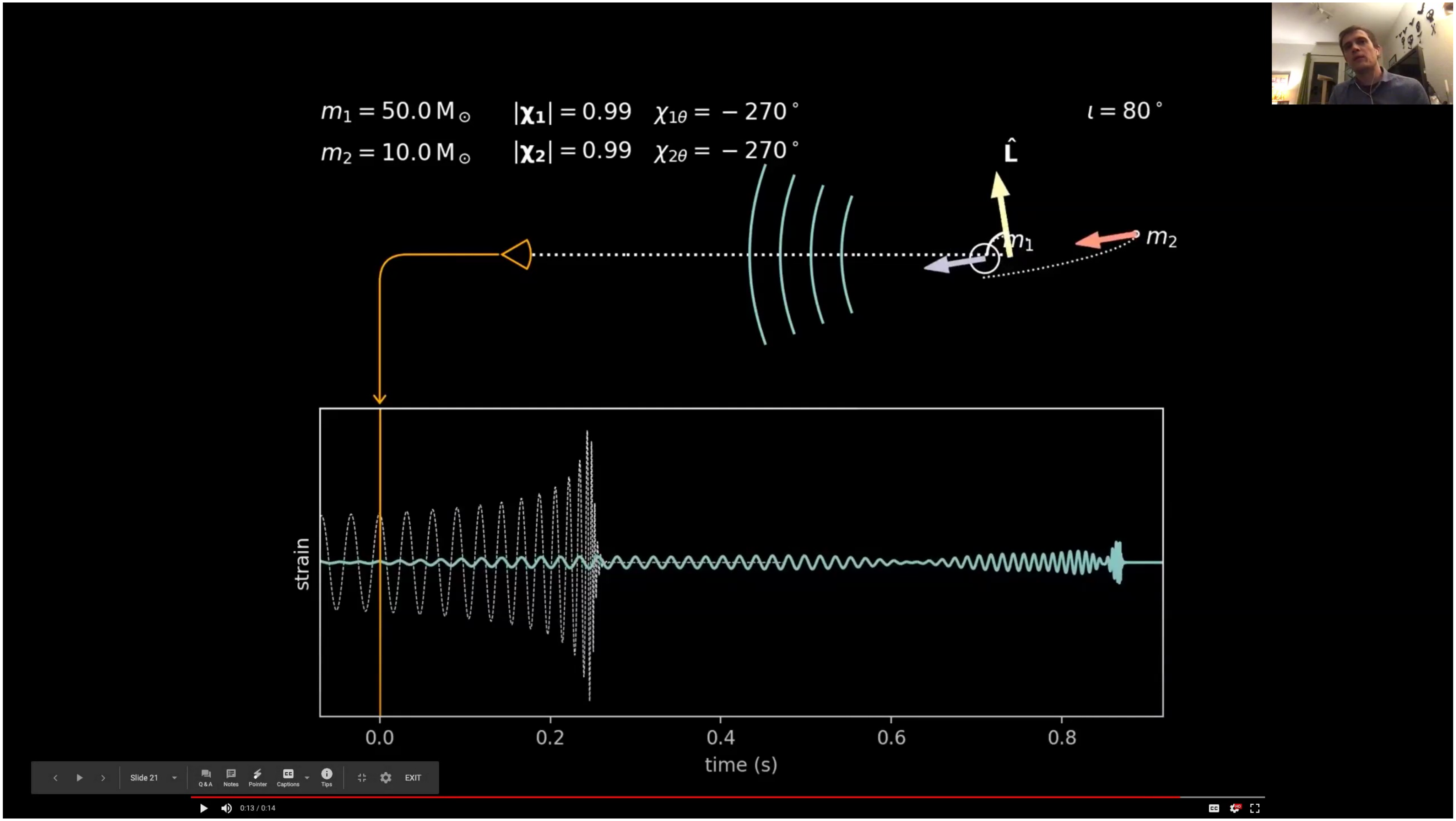
$m_1 = 50.0\,M_\odot$
$|\chi_1| = 0.99$
$\chi_{1\theta} = -270^\circ$
$\iota = 80^\circ$
$m_2 = 10.0\,M_\odot$
$|\chi_2| = 0.99$
$\chi_{2\theta} = -270^\circ$
$\hat{L}$
m_1
m_2
strain
0.0
0.2
0.4
0.6
0.8
time (s)
Slide 21
EXIT
0:13 / 0:14

Bayes' Theorem

- Bayesian inference is used to estimate GW's source parameters.
- Assume a signal *h* exists in some data *d*.
- Probability that the signal has parameters $\vartheta = \{m_1, m_2, \ldots\}$ is:

$$p(\vec{\vartheta}|d,h) = \frac{p(d|\vec{\vartheta},h)\,p(\vec{\vartheta}|h)}{p(d|h)}$$

- Prior: Represents our state of knowledge about the true parameters *before* measuring the data
- Likelihood: The probability of observing the data assuming that a particular set of parameters is true.
- Posterior: Represents our state of knowledge about the parameters *after* measuring the data.

Bayes' Theorem

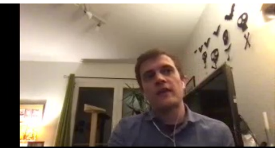

- Bayesian inference is used to estimate GW's source parameters.
- Assume a signal *h* exists in some data *d*.
- Probability that the signal has parameters $\vartheta = \{m_1, m_2, \ldots\}$ is:

$$p(\vec{\vartheta}|d,h) = \frac{p(d|\vec{\vartheta},h)\,p(\vec{\vartheta}|h)}{p(d|h)}$$

$$\text{Posterior} = \frac{\text{Likelihood} \quad \text{Prior}}{\text{Evidence}}$$

- **Prior**: Represents our state of knowledge about the true parameters *before* measuring the data
- **Likelihood**: The probability of observing the data assuming that a particular set of parameters is true.
- **Posterior**: Represents our state of knowledge about the parameters *after* measuring the data.

Evidence

$p(\vec{\vartheta}|d, h) = \frac{p(d|\vec{\vartheta}}{p}$

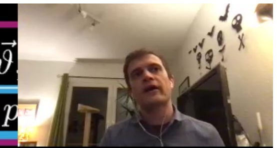

- Marginalizing the likelihood over all parameters yields the evidence:

$$p(d|h) = \int p(d|\vec{\vartheta}, h)p(\vec{\vartheta}|h)\mathrm{d}\vec{\vartheta}$$

The evidence can be used for model selection. Taking the ratio of evidences for two models yields the Bayes factor:

$$\mathcal{B}(A, B|d) = \frac{p(d|B)}{p(d|A)}$$

- A Bayes factor > 1 indicates model B is favored over model A

Likelihood

$p(\vec{\vartheta}|d,h) = p(d|\vec{\vartheta}$

- The likelihood function requires both a signal model and a noise model.
- In GW analyses it is common to assume wide-sense stationary (WSS) Gaussian noise. In that case:

$$\log p(d|\vec{\vartheta}, h) \propto -\frac{1}{2} \sum_{i=1}^{N_d} \left\langle d_i - h_i(\vec{\vartheta}),\, d_i - h_i(\vec{\vartheta}) \right\rangle$$

where:

$$\langle a,\, b \rangle = 4 \Re \int_0^\infty \frac{\tilde{a}^*(f)\tilde{b}(f)}{S_n(f)} \mathrm{d}f$$

Likelihood

$p(\vec{\vartheta}|d,h) = \frac{p(d|\vec{\vartheta} \ldots}{p \ldots}$

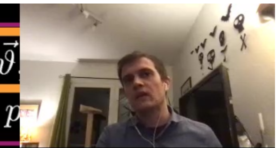

- The likelihood function requires both a signal model and a noise model.
- In GW analyses it is common to assume wide-sense stationary (WSS) Gaussian noise. In that case:

$$\log p(d|\vec{\vartheta}, h) \propto -\frac{1}{2}\sum_{i=1}^{N_d} \left\langle d_i - h_i(\vec{\vartheta}),\, d_i - h_i(\vec{\vartheta}) \right\rangle$$

where:

$$\langle a,\, b\rangle = 4\Re \int_0^\infty \frac{\tilde{a}^*(f)\tilde{b}(f)}{S_n(f)} \mathrm{d}f$$

Power Spectral Density (PSD)

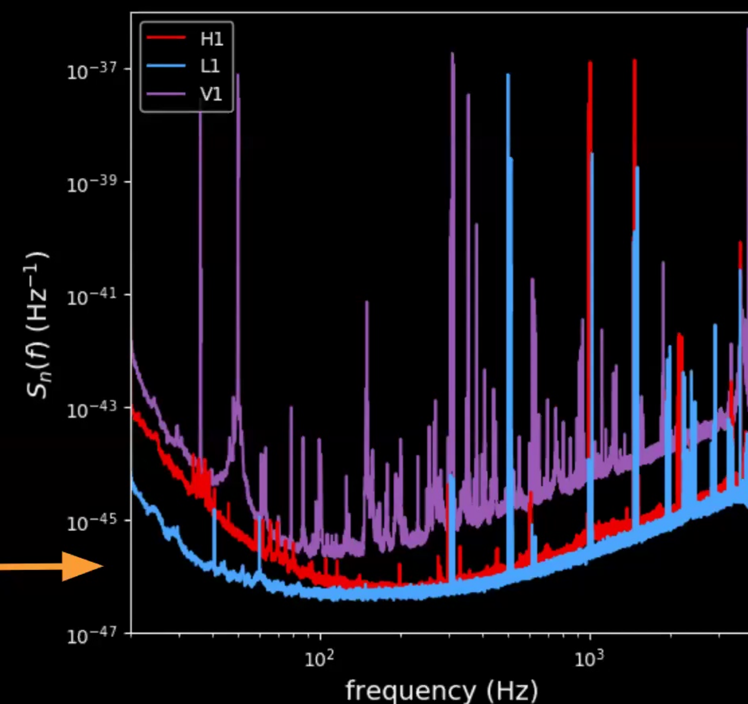

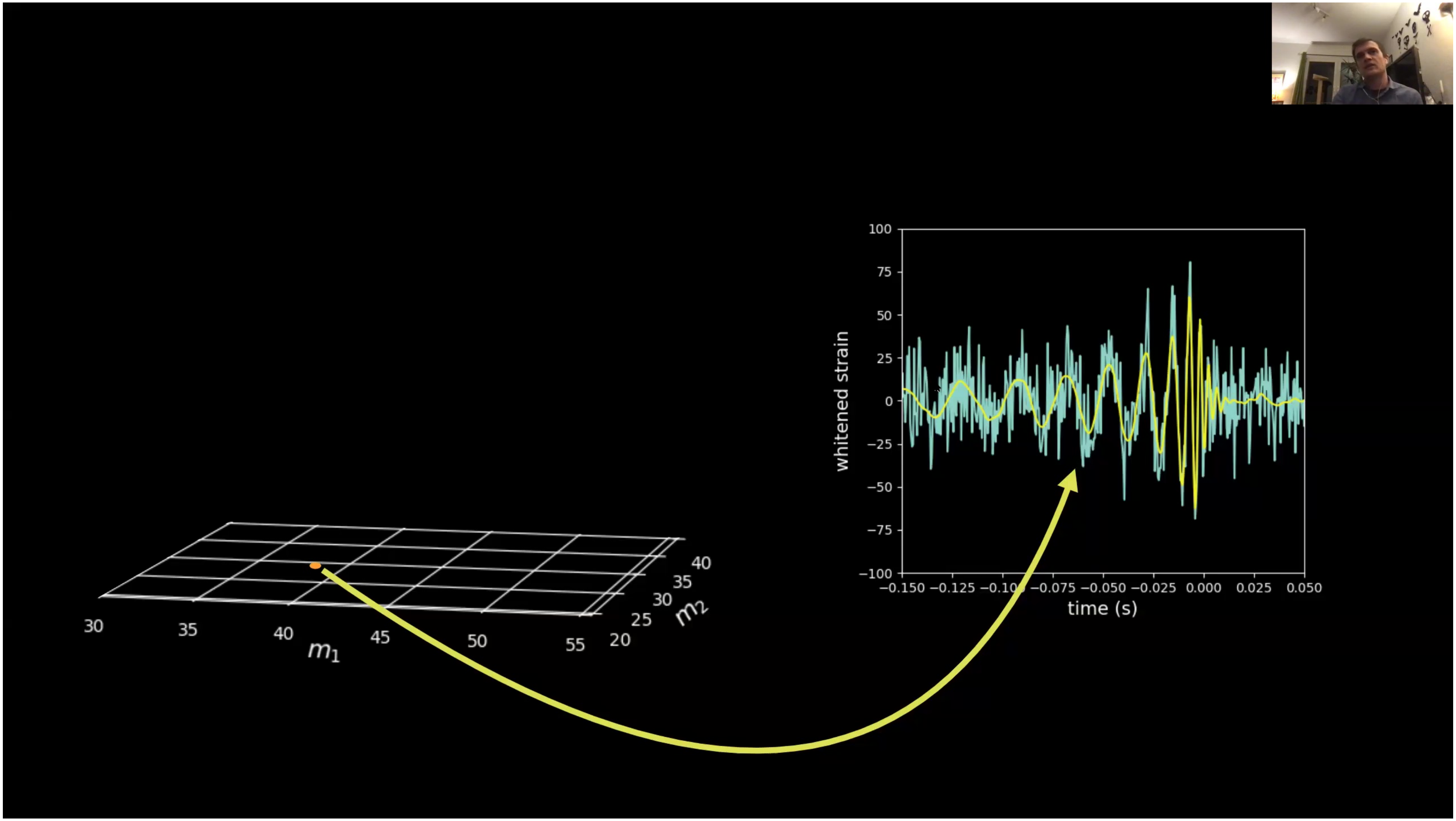
30
35
40
45
50
55
m_1
20
25
30
35
40
m_2
100
75
50
25
0
−25
−50
−75
−100
whitened strain
−0.150
−0.125
−0.075
−0.050
−0.025
0.000
0.025
0.050
time (s)

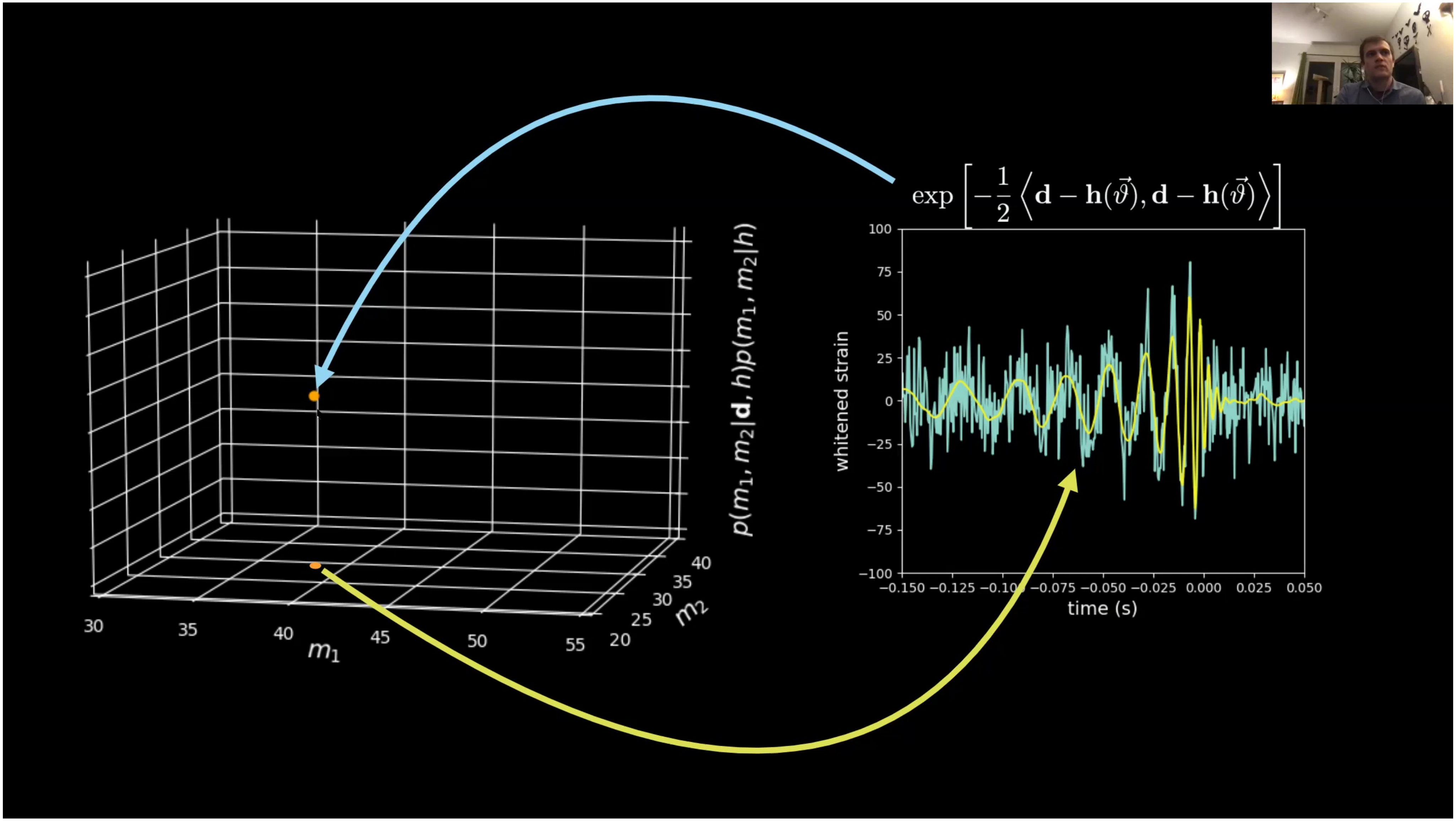

$\exp\left[-\frac{1}{2}\left\langle \mathbf{d}-\mathbf{h}(\vec{\vartheta}), \mathbf{d}-\mathbf{h}(\vec{\vartheta})\right\rangle\right]$
$p(m_1, m_2|\mathbf{d}, h)p(m_1, m_2|h)$
m_1
m_2
whitened strain
time (s)

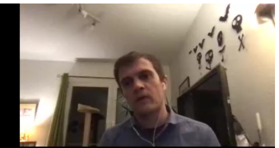

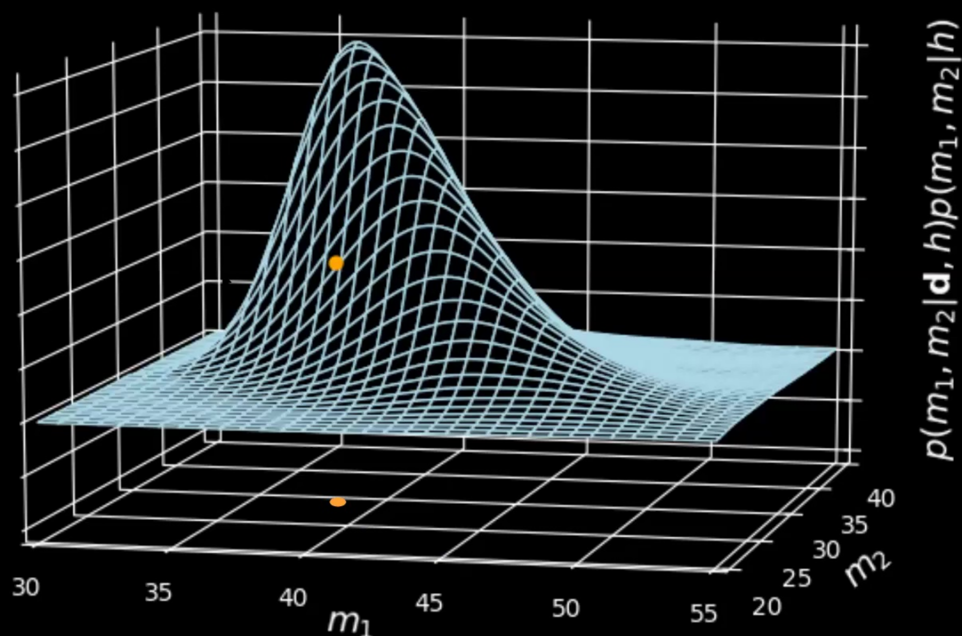

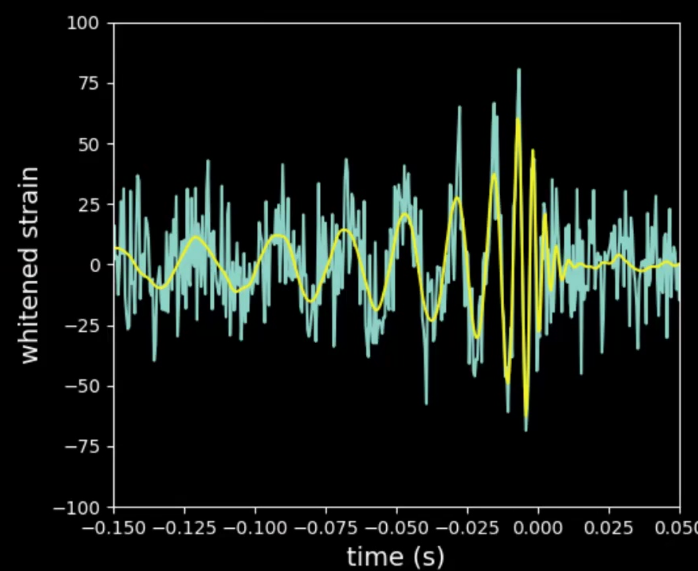

Stochastic samplers are used to sample the parameter space

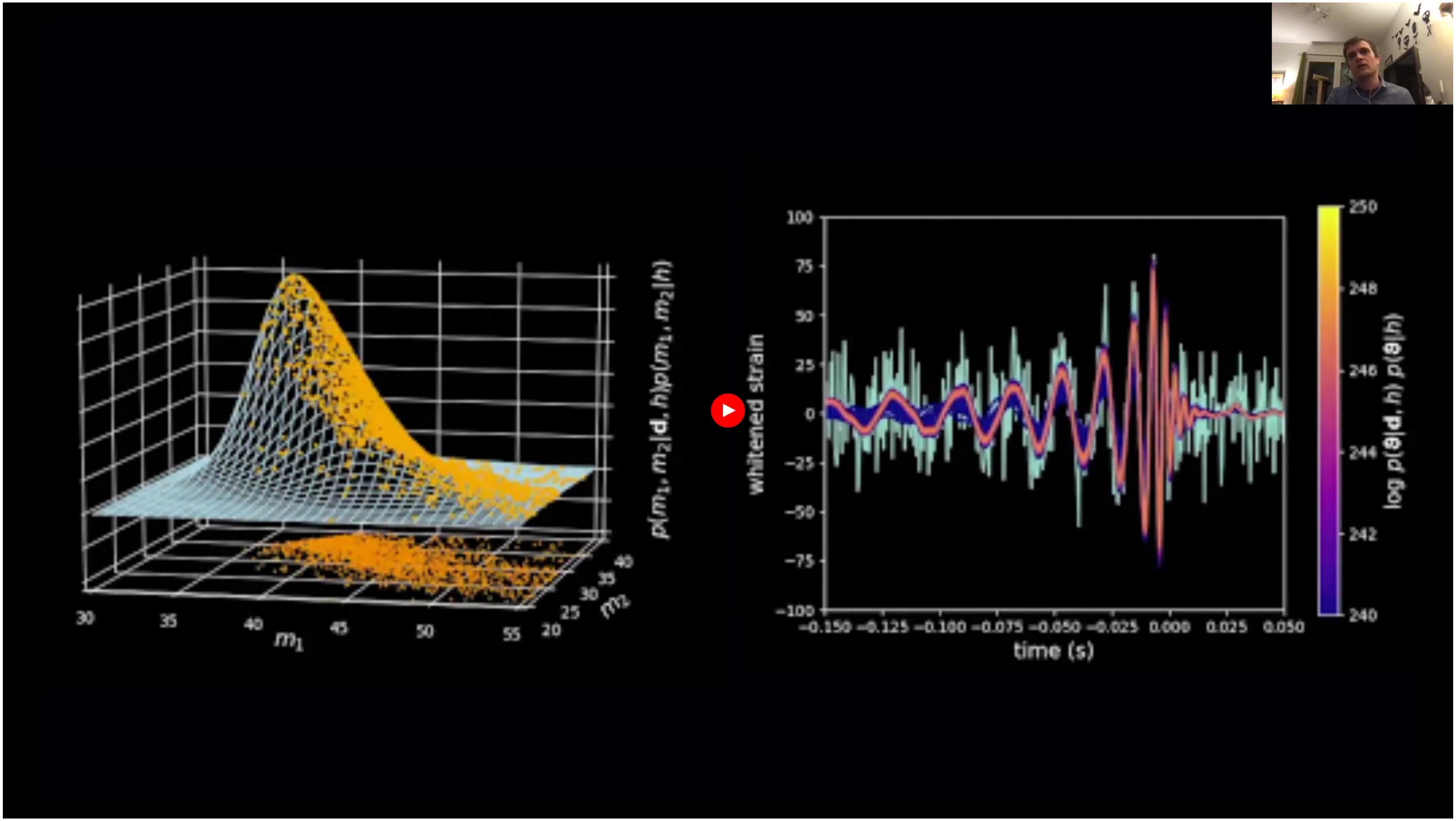

$p(m_1, m_2|\mathbf{d}, h)p(m_1, m_2|h)$
m_1
m_2
whitened strain
time (s)
log $p(\boldsymbol{\theta}|\mathbf{d}, h)$ $p(\boldsymbol{\theta}|h)$

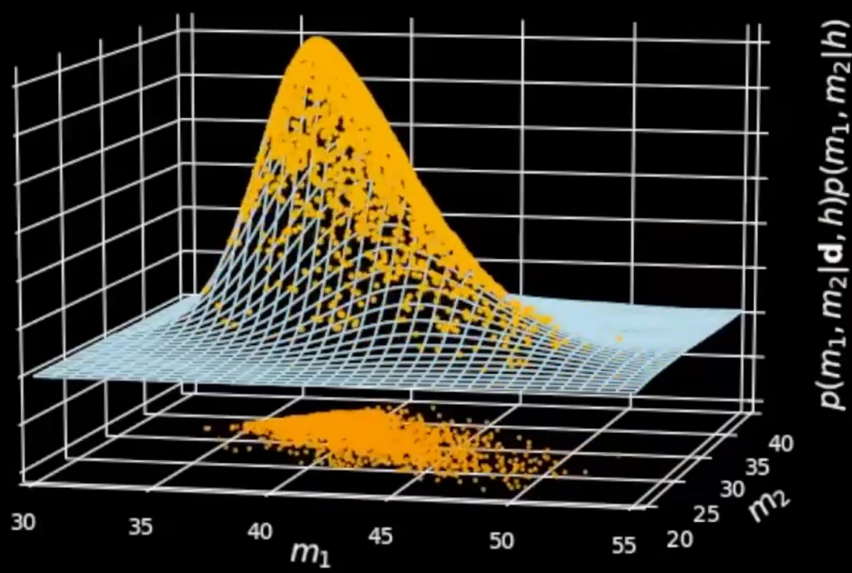
$p(m_1, m_2|\mathbf{d}, h)p(m_1, m_2|h)$
30
35
40
45
50
55
m_1
20
25
30
35
40
m_2

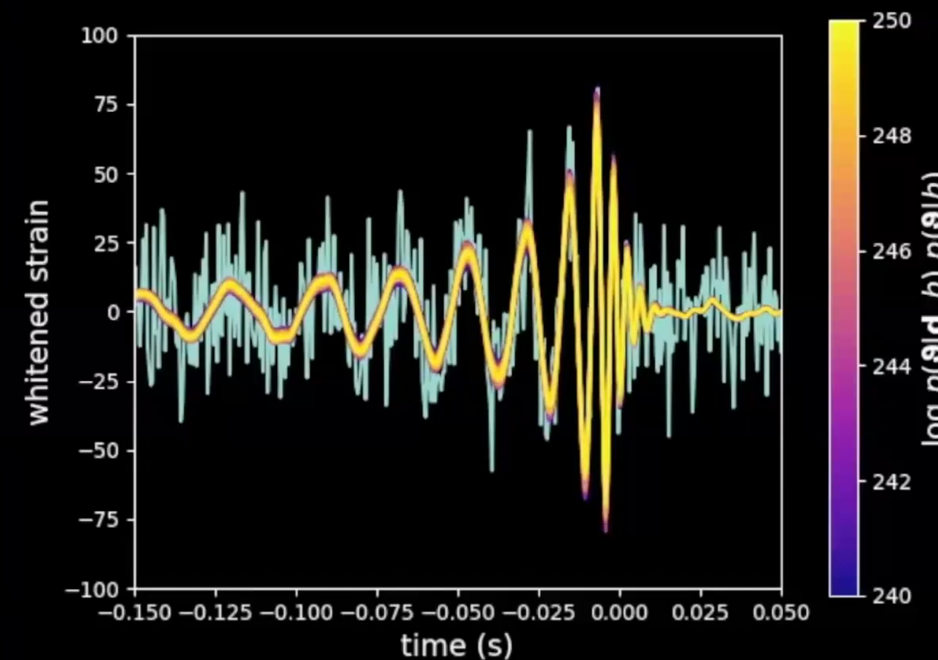
100
75
50
25
0
−25
−50
−75
−100
whitened strain
−0.150 −0.125 −0.100 −0.075 −0.050 −0.025 0.000 0.025 0.050
time (s)
250
248
246
244
242
240
$\log p(\boldsymbol{\vartheta}|\mathbf{d}, h)\ p(\boldsymbol{\vartheta}|h)$

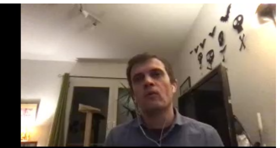

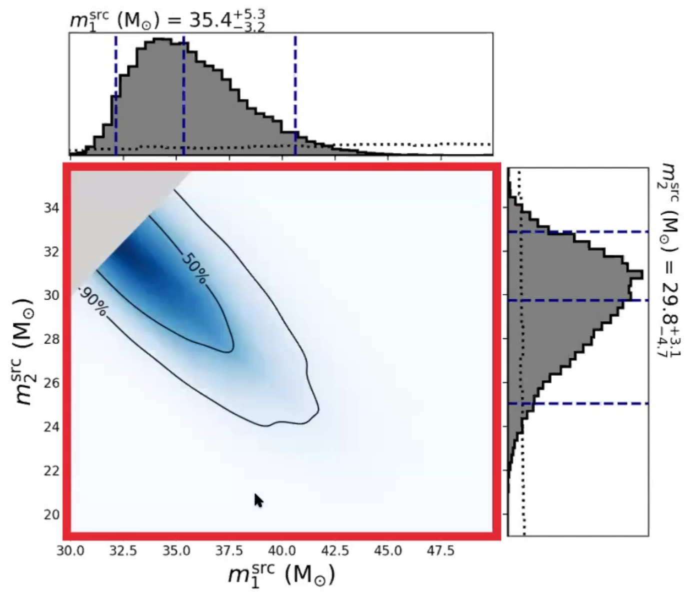

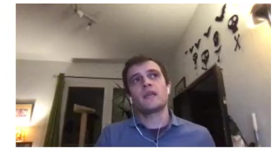

Example:
GW150914 posterior

A. Nitz & C. Capano, gwcatalog.org/top30_bbh

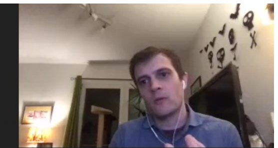

A complicated parameter space...

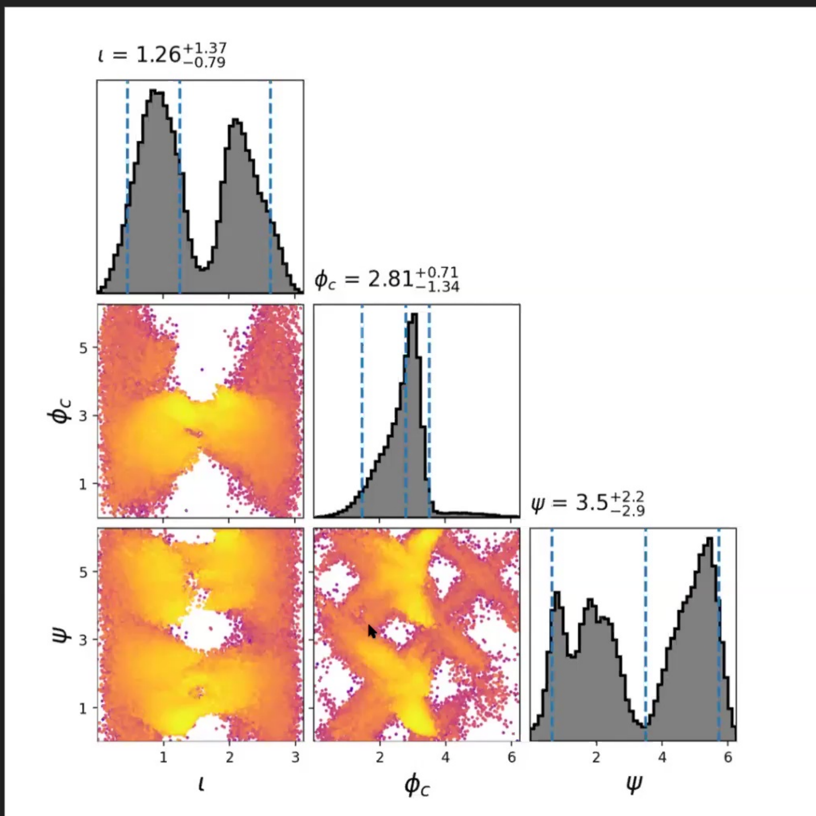

Numerically marginalized polarization

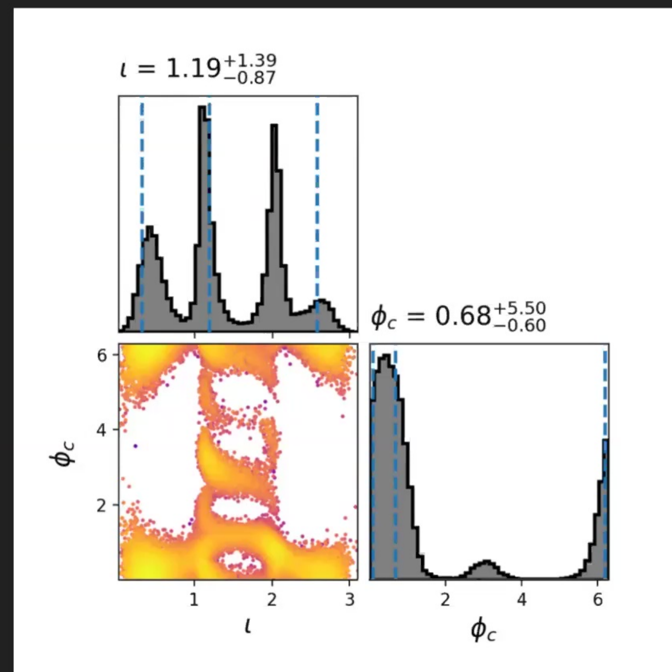

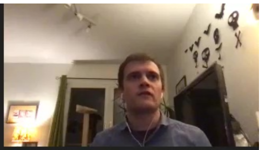

Our analysis

- Use PyCBC Inference with Dynesty nested sampler (20 - 40 000 live points)
- Two waveform models: IMRPhenomXPHM & NRSur7dq4
- Assume circular orbits
- Prior:
  - Uniform in comoving volume, isotropic sky location
  - Isotropic in orientation
  - Spins: isotropic in orientation, uniform in magnitude in [0, 0.99)
- Try two mass priors:
  - uniform in source-frame total mass & mass ratio* q
  - uniform in source-frame component masses

*We define $q \geq 1$

Results: Mass prior comparison

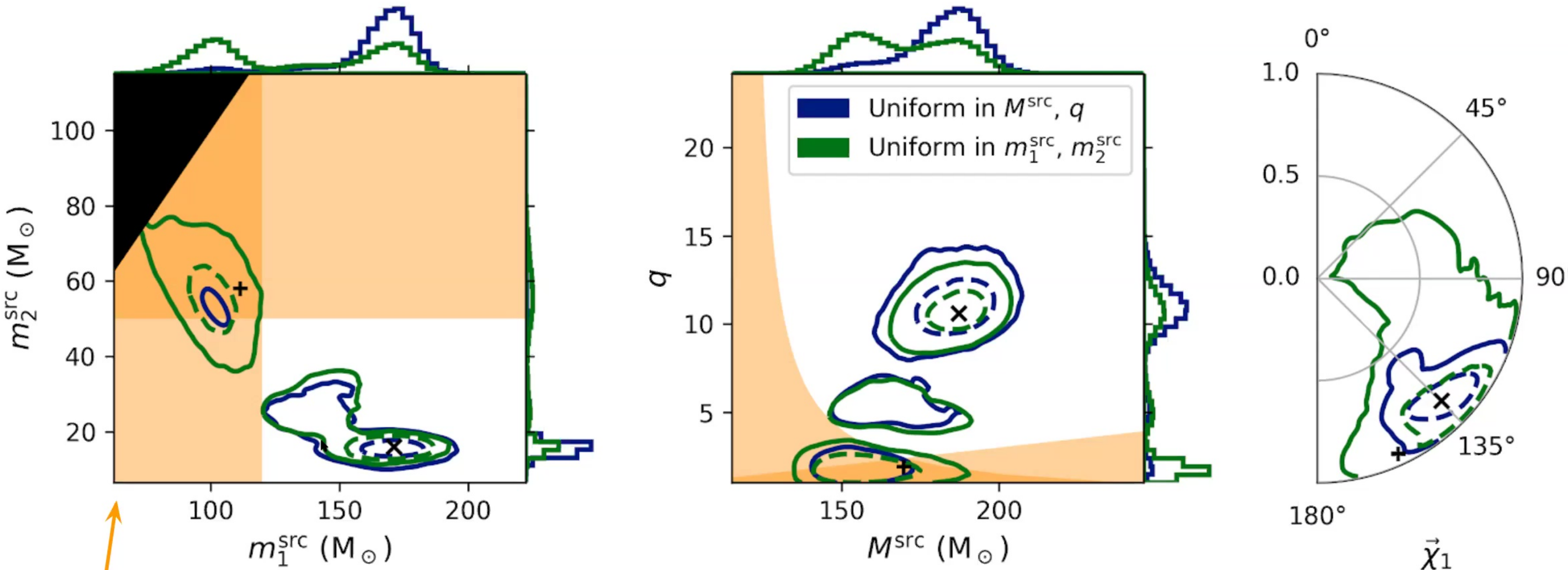

Orange regions indicate expected PISN mass gap

We find posterior support at q ~11 (m_1 ~170$M_\odot$, m_2 ~16$M_\odot$)

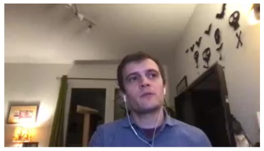

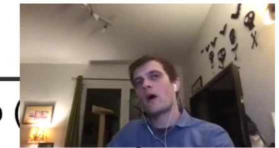

Likelihood surface

Signal-to-noise ratio (

$$\rho^* \equiv \sqrt{2(\text{likelihood ratio})}$$

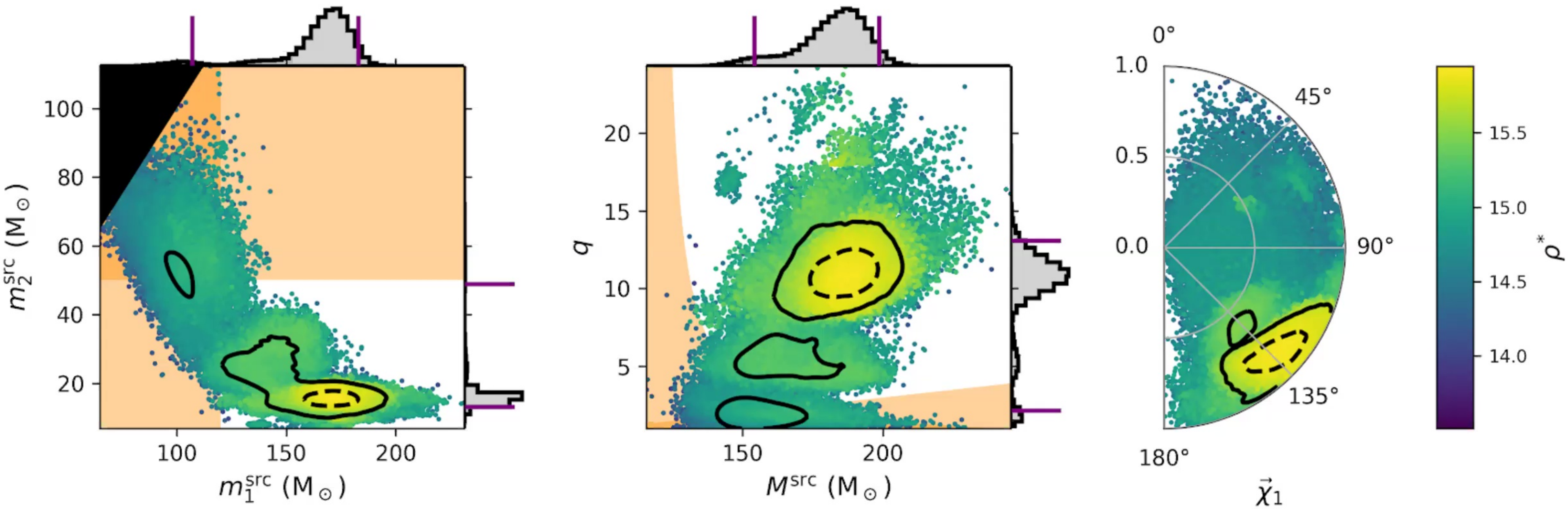

Waveform model: IMRPhenomXPHM
Prior: Uniform in total mass and mass ratio

The maximum likelihood waveform parameters are m_1 ~170 $M_\odot$, m_2 ~16$M_\odot$

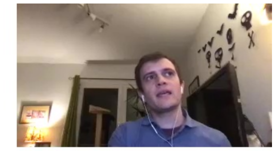

Results: Mass prior comparison

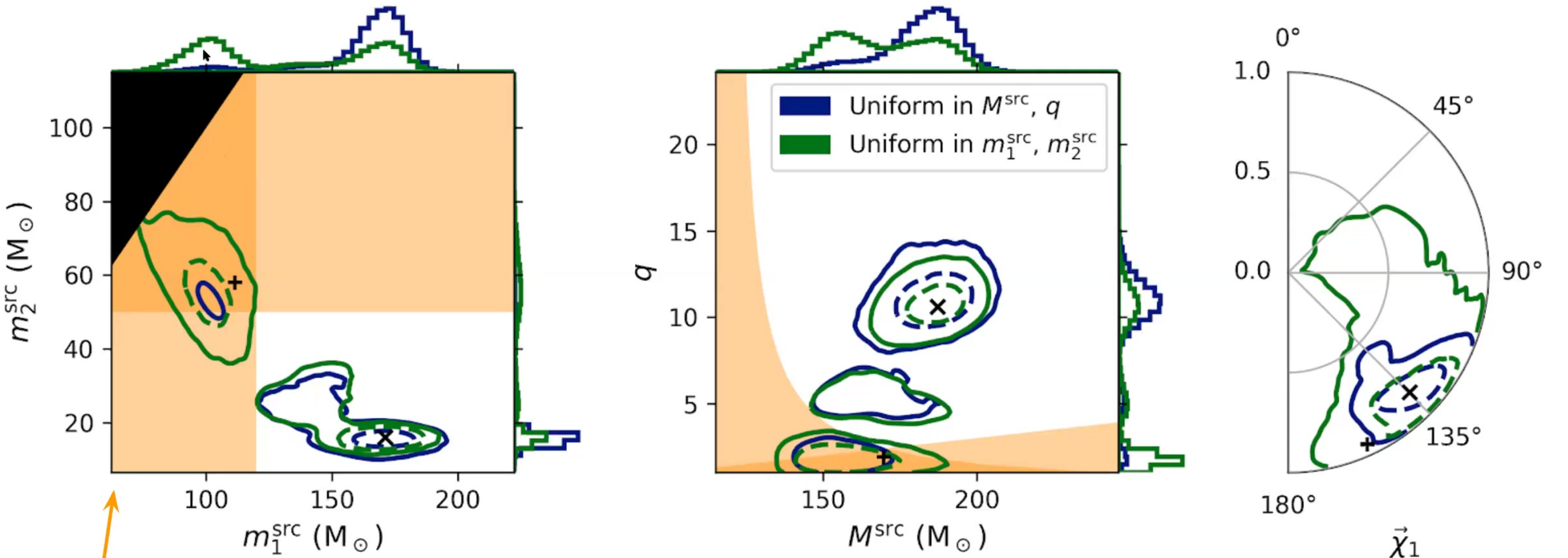

Orange regions indicate expected PISN mass gap

We find posterior support at q ~11 (m_1 ~170$M_\odot$, m_2 ~16$M_\odot$)

Likelihood surface

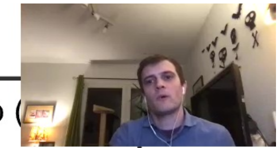

Signal-to-noise ratio (

$$\rho^* \equiv \sqrt{2(\text{likelihood ratio})}$$

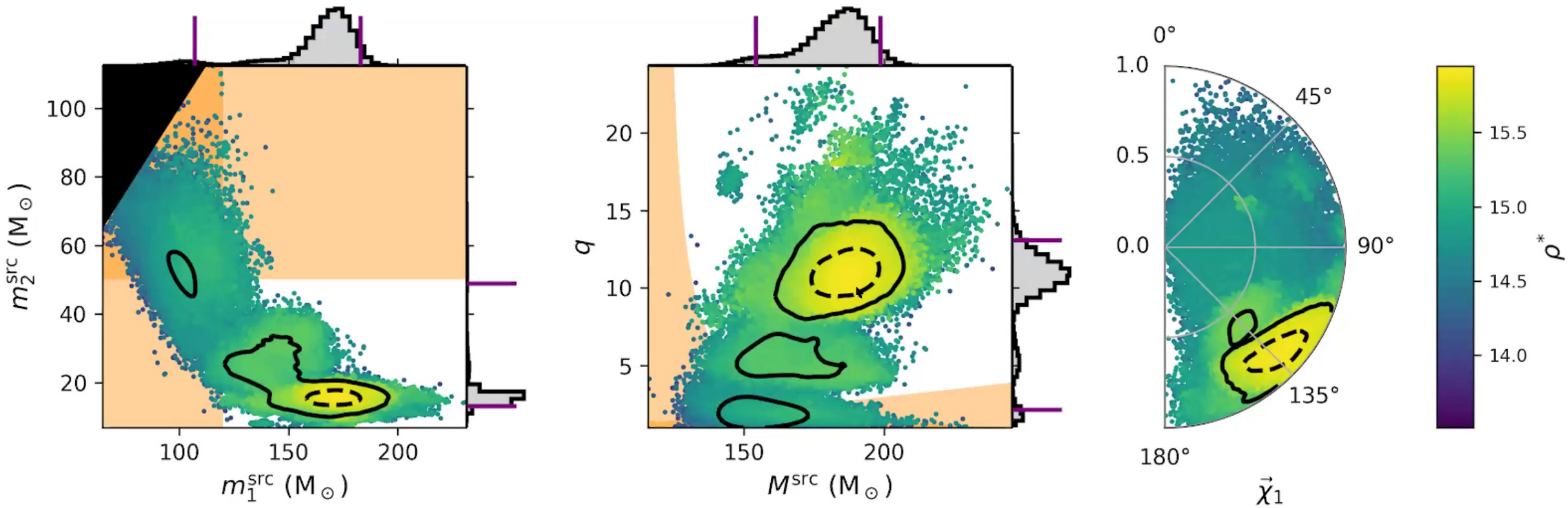

Waveform model: IMRPhenomXPHM
Prior: Uniform in total mass and mass ratio

The maximum likelihood waveform parameters are m_1 ~170 $M_\odot$, m_2 ~16$M_\odot$

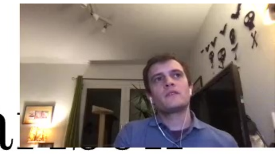

Waveform compa

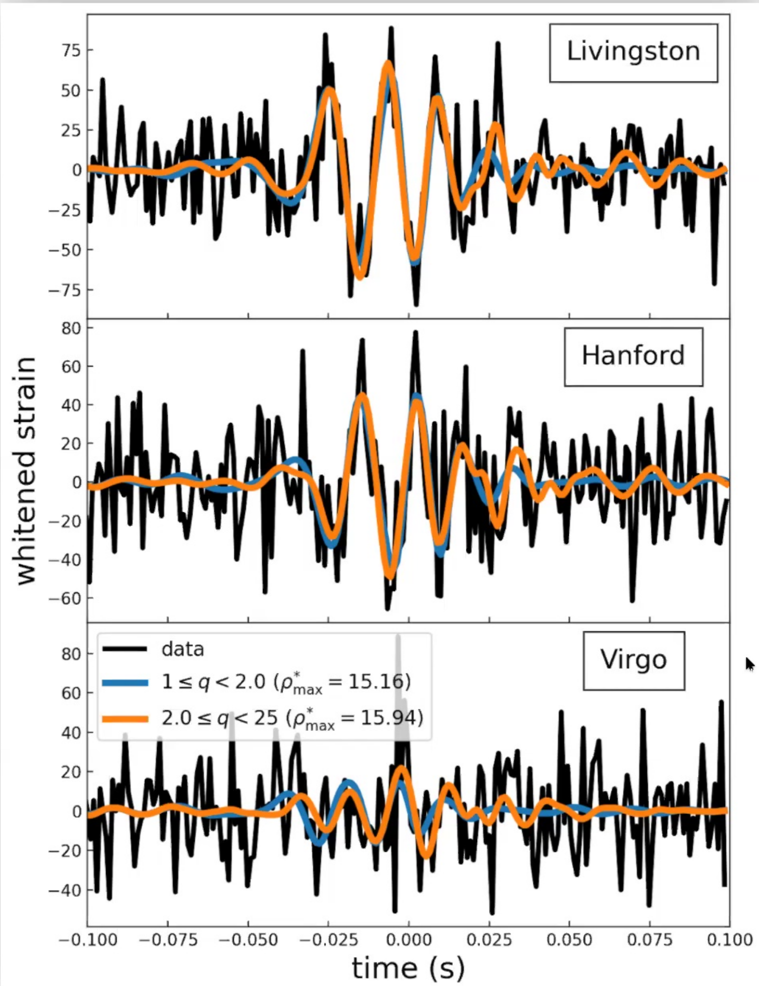

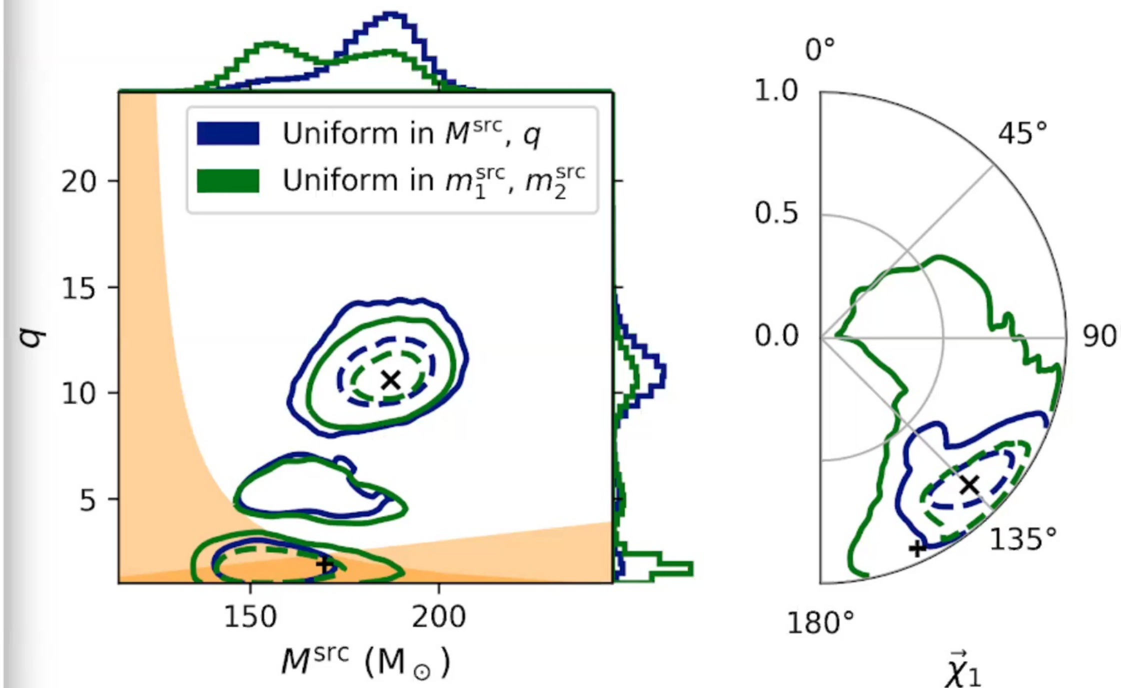

- Orange line / cross: maximum likelihood waveform
- Blue line / plus: max L waveform in q < 2 region

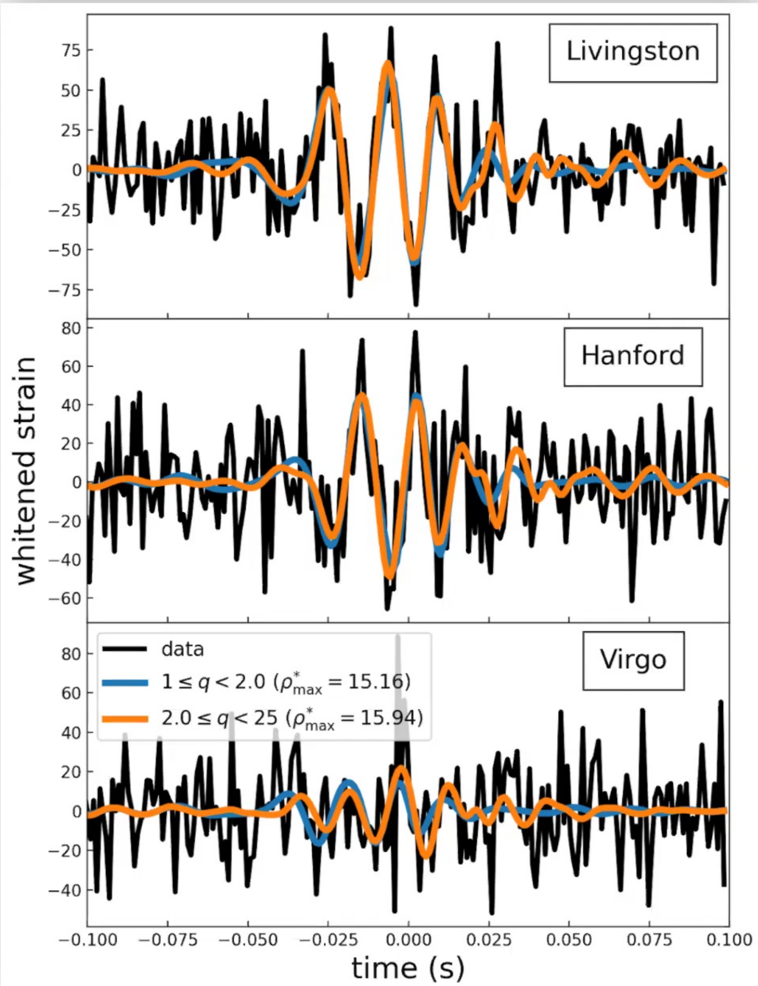

Sub-dominant harm

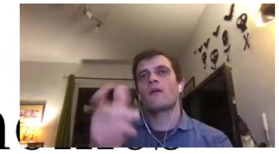

- GW is a sum of spin-weighted spherical harmonics:

$$h(t) = \Re\left\{(F_+ + iF_\times)\left(\sum_{\ell m} {}_{-2}Y_{\ell m}\mathfrak{h}_{\ell m}(t)\right)\right\}$$

- Dominant harmonic is (l, m) = (2, 2)
  - Only two previous events, GW190814 & GW190412, had measureable sub-dominant modes
- The q < 2 (blue line) and q > 2 (orange line) max L waveforms have ~ the same SNR from the dominant mode (14.3 and 14.5), but total SNR is 15.16 and 15.94, respectively.
- **Nearly all the additional SNR in the q > 2 waveform is from sub-dominant modes.**

Results using NR Surrogate model

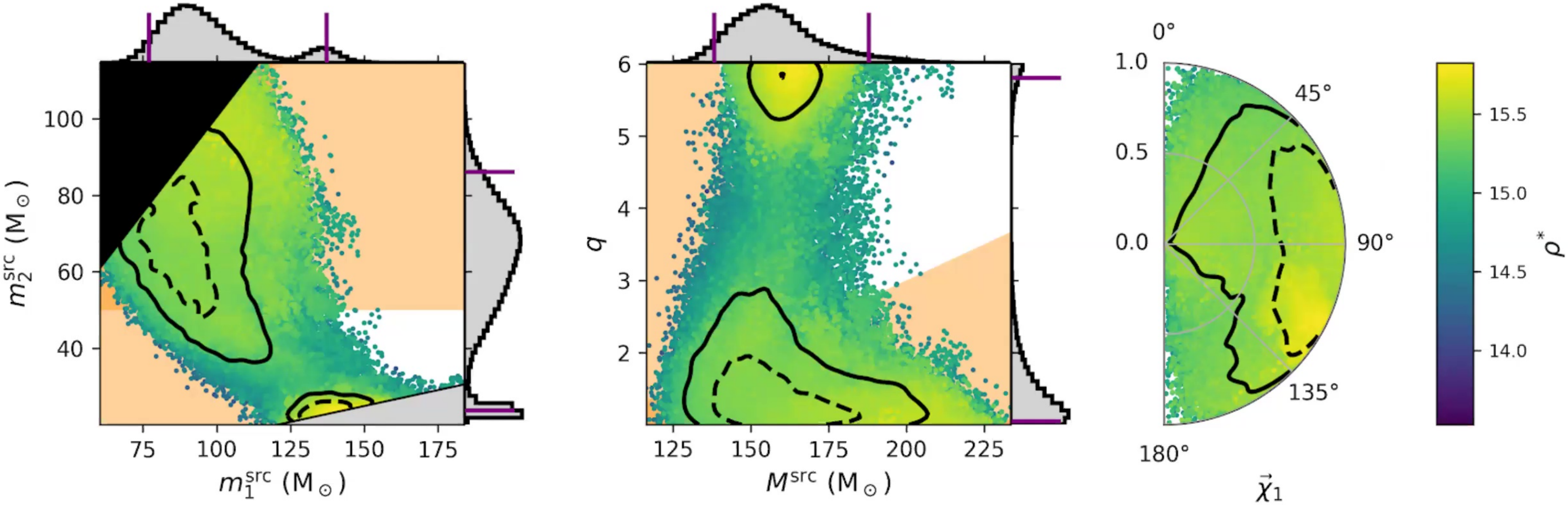

Waveform model: NR Surrogate (NRSur7dq4)
Prior: Uniform in total mass and mass ratio

Constrained EM analysis

- We also evaluate posterior assuming the ZTF flair & GW190521 were from the same source
- Repeat analysis fixing the sky location and distance to location of the flair found by ZTF
- Results shown for uniform in total mass and mass ratio prior (compares to previous two slides)

Constrained EM results

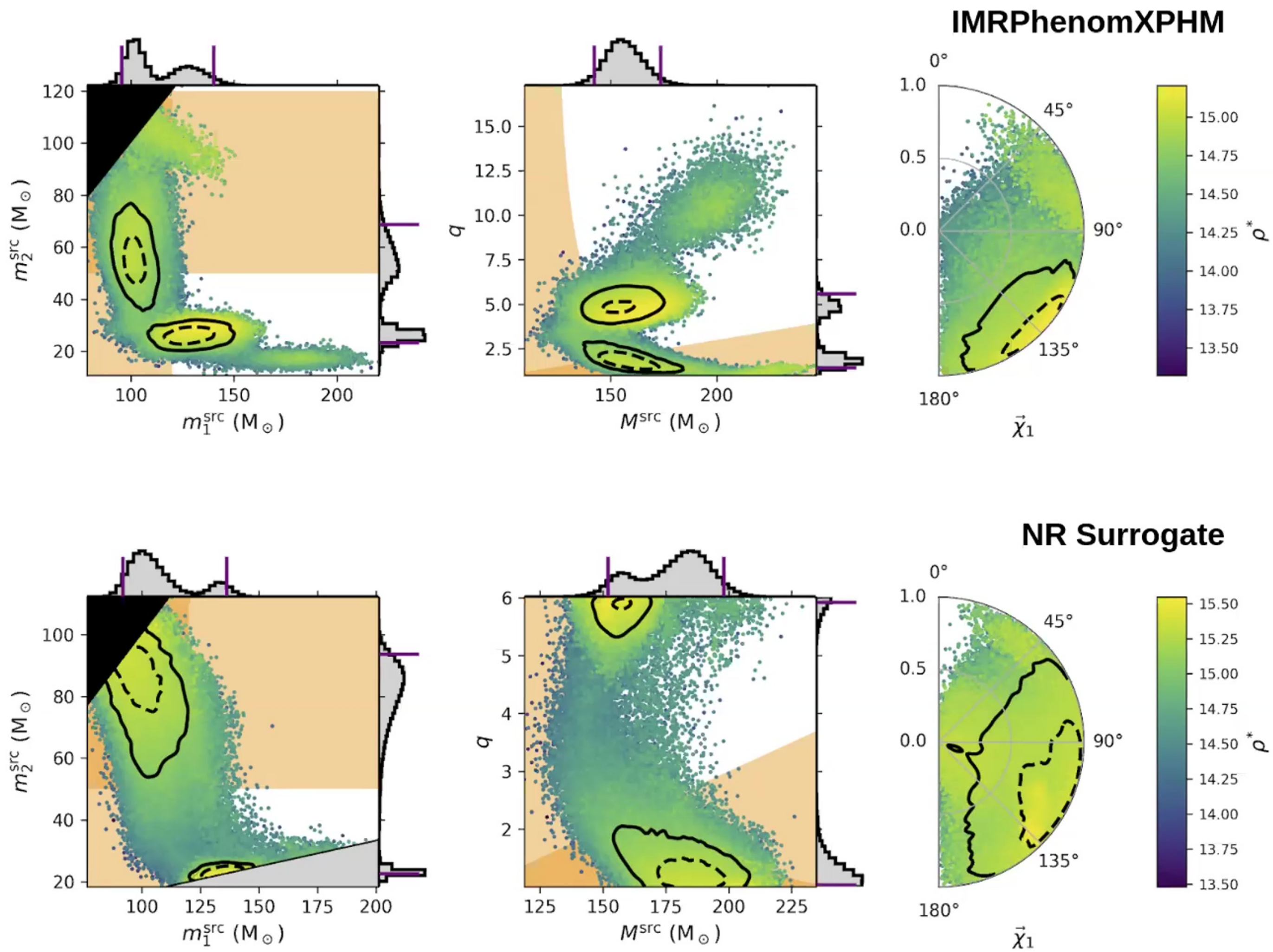

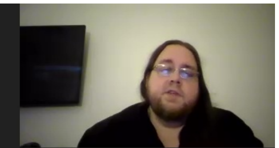

Constrained EM results

- Highest mass ratio mode is disfavored
  - The redshift constraint is largely inconsistent with the distance required for this mode
- Evidence for spatial coincidence?
  - Note: time coincidence is excluded
  - Range of assumptions depending on selection effects
    - (1) assume unbiased all-sky observation out to furthest redshift we consider
      - ln B ~ 2.3
    - (2) assume targeted observation of low-latency region
      - ln B ~ -4
  - Possible corroboration from recurrence of flare in the future

Implications

- Support for higher-mass-ratio modes indicates that neither component is necessarily within the PISN (50-120 solar mass) range
  - Both components could have formed as a direct remnant (still need to explain high spin of primary)
- Primary spin angle is suggestive of a dynamical formation
  - Consistent with forming within an AGN
- If a common origin with the EM flare can be confirmed the highest mass ratio is nearly excluded
  - Remaining support comparable between lowest mass ratio and q ~ 5-6 mode.

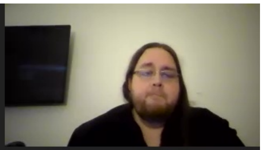

Prior Results and Systematics

Slide 42 Q & A Notes Pointer Captions Tips EXIT

Differences from LVC analysis

- The LVC reported masses of $m_1 = 85^{+21}_{-14} M_\odot$ and $m_2 = 66^{+17}_{-18} M_\odot$
- Several differences between their analysis and ours
- Waveform models: LVC used IMRPhenomPv3HM, SEOBNR, NRSur7dq4
- Different sampling methods:
  - LVC used LALInference
  - No numerical marginalization over phase and polarization
- Different priors:
  - LVC: uniform in detector-frame masses and uniform in luminosity volume
- LVC applied cuts to detector-frame masses
  - detector-frame total mass > 200 $M_\odot$
  - 70 $M_\odot$ < detector-frame chirp mass < 150 $M_\odot$
  - mass ratio < 6
  - $m_2 > 30 M_\odot$

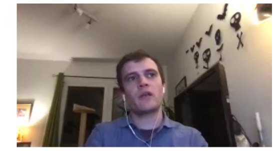

Comparison to LVC results

Prior: uniform in **source-frame masses**,
uniform in **comoving volume**

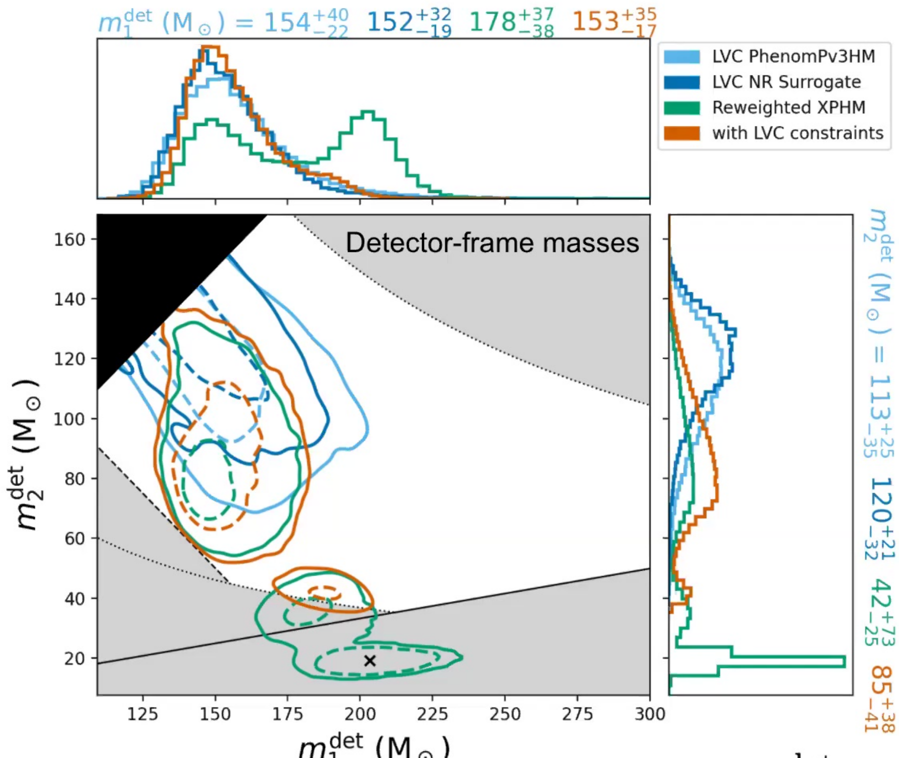

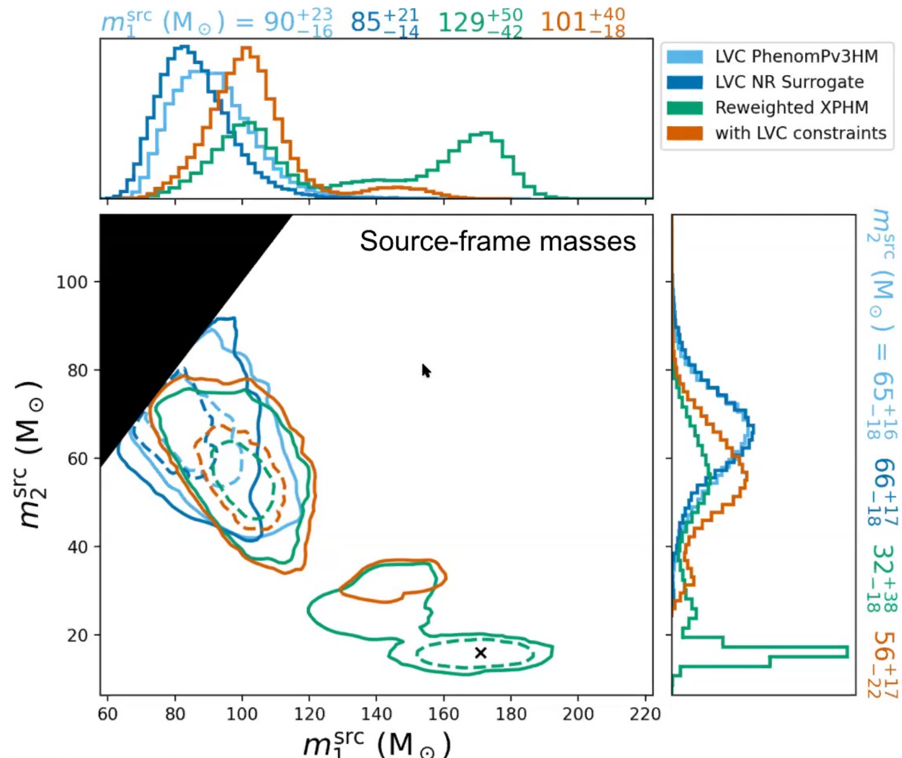

$$m^{\rm det}_{(1,2)} = m^{\rm src}_{(1,2)}(1+z)$$

Comparison to LVC results

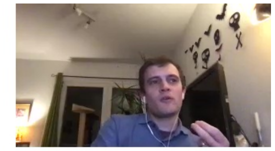

Prior: uniform in **detector-frame masses**,
uniform in **cubic luminosity distance**

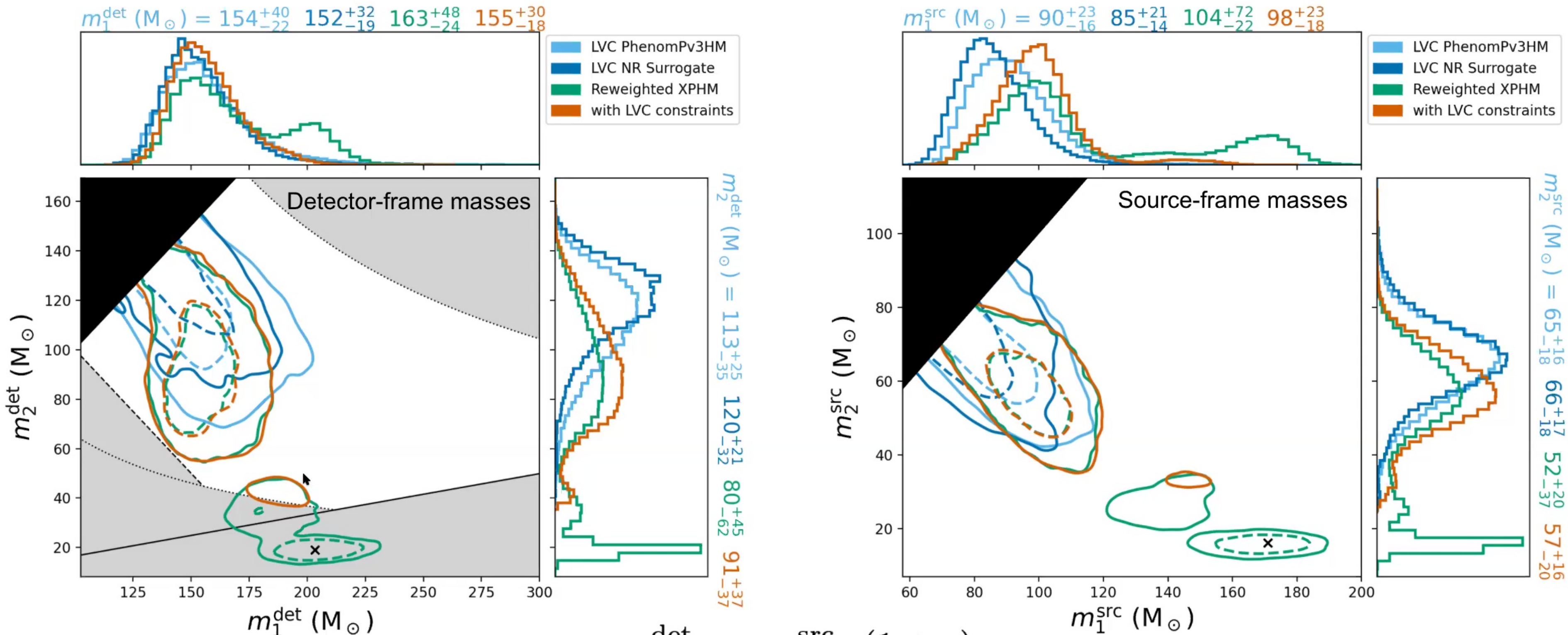

$$m^{\text{det}}_{(1,2)} = m^{\text{src}}_{(1,2)}(1+z)$$

Why are our results different from the LVC results?

- Short answer: the parameter space cuts (especially the chirp mass cut) excluded the higher mass ratio mode

- Why were these cuts chosen?
  - More efficient to sample restricted parameter space
  - Region seemed suitable likely due to uniform in detector-frame masses and cubic distance prior, combined with complicated multimodal structure of likelihood surface

- Different waveform models, sampling techniques, and priors used make it difficult to say conclusively, however

GW190521: A continuing mystery

- Could this be a non-circular merger?
- Are the waveform models suitably understood to minimize systematics?
- More NR simulations and models that include all physical effects (eccentricity, large mass ratio, high spin) are needed to better understand this event

Thank you!

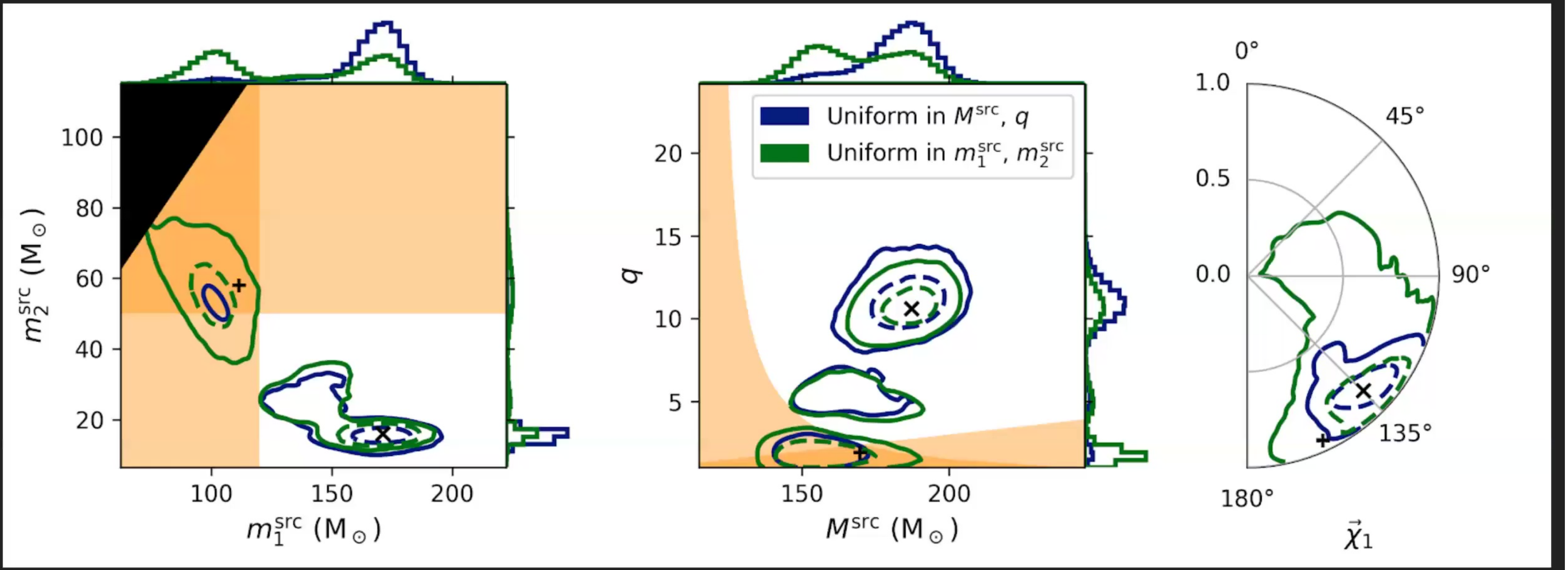

Uniform in M^{src}, q
Uniform in m_1^{src}, m_2^{src}
m_2^{src} ($M_\odot$)
m_1^{src} ($M_\odot$)
q
M^{src} ($M_\odot$)
$\vec{\chi}_1$
0°
45°
90°
135°
180°